




Article

Enhancing Bioenergy Production from *Chlorella* via Salt-Induced Stress and Heat Pretreatment

Themistoklis Sfetsas ^{1,2,*}, Sopio Ghoghoberidze ² , Petros Samaras ³ , Polycarpos Falaras ⁴  and Thomas Kotsopoulos ^{1,*} 

¹ Department of Hydraulics, Soil Science and Agricultural Engineering, School of Agriculture, Aristotle University of Thessaloniki, 54124 Thessaloniki, Greece

² Qlab Private Company, Research & Development, Quality Control and Testing Services, 57008 Thessaloniki, Greece; sghogho@elgo.gr

³ Laboratory of Technologies for Environmental Protection and Utilization of Food By-Products, Department of Food Science and Technology, International Hellenic University (IHU), Sindos, 57400 Thessaloniki, Greece; samaras@ihu.gr

⁴ Institute of Nanoscience and Nanotechnology, National Center of Scientific Research “Demokritos”, Agia Paraskevi, 15310 Athens, Greece; p.falaras@inn.demokritos.gr

* Correspondence: tsfetsas@agro.auth.gr (T.S.); mkotsop@agro.auth.gr (T.K.)

Abstract: This study presents an integrated strategy to optimize biofuel production from *Chlorella sorokiniana* (CSO) and *Chlorella vulgaris* (CVU) by combining salt-induced stress and thermal pretreatment. The microalgae were cultivated in anaerobic digestate effluent (ADE) under stress and non-stress conditions to evaluate nutrient availability’s impact on biomass composition. Salt stress significantly enhanced lipid accumulation, with CVU exhibiting a 51.6% increase. Thermal pretreatment of biomass at 90 °C for 10 h achieved the highest methane yield (481 mL CH₄/g VS), with CVU outperforming CSO. Milder pretreatment conditions (40 °C for 4 h) were more energy-efficient for CSO, achieving a yield of 2.67%. Fatty acid profiles demonstrated species-specific biodiesel properties, with CSO rich in oleic acid (33.47%) offering enhanced oxidative stability and cold flow performance, while CVU showed a higher polyunsaturated fatty acid content. This research highlights the economic viability of using ADE as a low-cost cultivation medium and the potential for scalable thermal pretreatments. Future research should focus on reducing energy demands of pretreatment processes and exploring alternative stress induction methods to further enhance biofuel yields. These findings offer valuable insights for tailoring cultivation and processing strategies to maximize lipid and methane production, supporting sustainable and economically viable dual biofuel production systems.

Keywords: microalgae (MA); anaerobic digestion effluent (ADE); biodiesel; *C. sorokiniana*; *C. vulgaris*; biogas potential



Academic Editor: Jorge Costa

Received: 17 February 2025

Revised: 9 March 2025

Accepted: 19 March 2025

Published: 27 March 2025

Citation: Sfetsas, T.; Ghoghoberidze, S.; Samaras, P.; Falaras, P.; Kotsopoulos, T. Enhancing Bioenergy Production from *Chlorella* via Salt-Induced Stress and Heat Pretreatment. *Fuels* **2025**, *6*, 23. <https://doi.org/10.3390/fuels6020023>

Copyright: © 2025 by the authors. Licensee MDPI, Basel, Switzerland. This article is an open access article distributed under the terms and conditions of the Creative Commons Attribution (CC BY) license (<https://creativecommons.org/licenses/by/4.0/>).

1. Introduction

The pursuit of renewable and sustainable energy sources has accelerated research into microalgae as promising biofuel feedstocks. Species such as *Chlorella vulgaris* (CVU) and *Chlorella sorokiniana* (CSO) are valued for their rapid growth rates, adaptability to diverse environments (e.g., wastewater), and nutrient-dense composition, making them ideal candidates for bioenergy applications [1–3]. Besides biofuel production, microalgae offer significant environmental benefits, including reduced competition for land with food crops and bioremediation capabilities in wastewater treatment [2]. Despite their potential, microalgal biofuel production faces several challenges, including high cultivation costs,

low lipid yields under normal growth conditions, and energy-intensive harvesting and pretreatment processes [4–9]. Furthermore, the robust cell walls of microalgae limit lipid extraction efficiency, requiring innovative strategies to overcome these limitations and improve biofuel recovery [10–12].

The conversion of microalgal biomass into biofuels is significantly challenged by the presence of robust cell wall structures, composed of complex polysaccharides and polymers such as cellulose, hemicellulose, and sporopollenin-like materials [13,14]. This structural resilience, while beneficial for the organism's survival, restricts microbial degradation and nutrient accessibility, which are critical for biofuel recovery. Overcoming these barriers requires specific pretreatment strategies to enhance solubilization of cell wall components, thereby improving intracellular nutrient access and maximizing methane and biodiesel yields [15].

Among biofuel production methods, methane production through anaerobic digestion is a promising approach due to its ability to utilize microalgal biomass as a renewable substrate [16,17]. The biochemical methane potential (BMP) test is widely used to evaluate the efficiency of methane production, serving as a key indicator of bioenergy potential [18,19].

Factors such as the biochemical composition of microalgal biomass, pretreatment techniques, microbial inoculum type, and substrate-to-inoculum (S/I) ratio play pivotal roles in determining BMP (Biochemical Methane Potential) outcomes in anaerobic digestion (AD). High protein and lipid contents in microalgae typically enhance methane production, but a low carbon-to-nitrogen (C/N) ratio, common in microalgal biomass due to high nitrogen content, can lead to ammonia production that inhibits methanogenic activity. Co-digestion with carbon-rich substrates, such as food or agricultural waste, has proven effective for balancing the C/N ratio, thereby improving both methane yield and AD stability [20,21].

Pretreatment of microalgal biomass is crucial to improving BMP by increasing microbial accessibility to resilient cell wall components. Enzymatic pretreatments targeting specific polymers, such as cellulase for cellulose and xylanase for hemicellulose, have shown promise, enhancing methane yields by up to 15% [22,23]. However, while mechanical and thermal pretreatments can also increase methane production, their high energy requirements often limit practical application [24,25].

Moreover, selecting the appropriate microbial inoculum is essential for optimizing BMP. Anaerobic inocula, specifically adapted for microalgal biomass degradation, demonstrates improved BMP efficiency. Thermophilic conditions combined with inocula enriched with Clostridia and hydrogenotrophic methanogens can enhance hydrolytic and methanogenic activity, reducing the need for energy-intensive pretreatments and emphasizing the importance of microbial adaptation for effective BMP [23,26].

A range of pretreatment methods, including thermal, chemical, enzymatic, and acid-thermal techniques, have been evaluated to optimize microalgal biomass for biofuel production. Thermal pretreatment at elevated temperatures is particularly effective, breaking down complex cell wall components and releasing carbohydrates, leading to increases in methane production by up to 108% under optimal conditions [25,27]. However, thermal pretreatment alone may not fully disrupt cell walls in more resilient microalgae species, prompting the use of supplementary chemical agents. For example, combining thermal pretreatment with acidic or alkaline conditions selectively targets macromolecules like proteins or carbohydrates, facilitating their degradation and increasing the availability of fermentable sugars [20,28]. Acid-thermal pretreatment, which involves dilute sulfuric acid at high temperatures, is effective in solubilizing carbohydrates, crucial for maximizing methane yields in anaerobic digestion and enhancing hydrogen production through fermentation pathways [27]. Conversely, alkaline-thermal pretreatment improves protein

solubilization and mitigates ammonia buildup during AD, preventing microbial inhibition and enhancing methane output [28]. Optimized pretreatment conditions can increase digestibility by up to 50% for CVU and by 21–27% for *Scenedesmus* sp., despite the latter's more resilient cell wall structure [20].

Thermal pretreatment is a critical step for enhancing the digestibility of microalgae biomass, particularly for biofuel production. While elevated temperatures, often exceeding 50 °C, have been widely studied, our approach intentionally explores lower ranges, specifically around 40 °C, as a safe and effective step. This temperature range aligns with mesophilic conditions and avoids the adverse effects of thermal denaturation while stimulating endogenous enzymatic activity. Carrillo-Reyes et al. [29] demonstrated that enzymatic pretreatments, including hydrolytic microbial consortia, disrupt complex cell walls efficiently without requiring high energy inputs. At 40 °C, specific biochemical changes are induced, such as the activation of cellulase, hemicellulase, and protease enzymes, which enhance the solubilization of carbohydrates, proteins, and lipids, facilitating microbial access to substrates and improving methane yields [30,31].

Unlike traditional thermal pretreatments exceeding 50 °C, our study's novelty lies in optimizing methane yields by leveraging mesophilic and sub-mesophilic processes, such as those at 20 °C and 40 °C. At 20 °C, biochemical pathways driven by natural microbial processes allow slow but sustained hydrolysis while minimizing energy consumption, offering a sustainable and cost-effective alternative [32]. Acid-thermal pretreatment, for example, has been effective at solubilizing carbohydrates with dilute sulfuric acid, and alkaline conditions mitigate ammonia buildup during anaerobic digestion (AD), improving methane yields by 21–27% for resilient species like *Scenedesmus* sp. [25,27,33].

Innovative physical methods such as cold atmospheric-pressure plasma (CAPP) have recently shown potential for enhancing lipid productivity and biodiesel yields. This method uses ionized gas to create reactive species that penetrate the cell wall, increasing lipid extraction efficiency without producing harmful residues. CAPP pretreatment is an environmentally sustainable alternative to traditional chemical methods, aligning with regulatory standards and supporting large-scale biodiesel production with minimal ecological impact. Given its non-mutagenic nature, CAPP is particularly suitable for applications in closed-loop cultivation systems, where preserving microalgal genetic integrity is essential [34].

Finally, optimizing pretreatment processes based on specific microalgal characteristics, desired biofuel type, and economic constraints is critical. While intensive thermal and chemical pretreatments enhance biofuel yield, they require substantial energy, potentially offsetting biofuel gains [25,35]. Recent studies suggest that alternative, lower-energy methods such as enzymatic or CAPP treatments, as well as hybrid approaches combining thermal and non-thermal techniques, may reduce energy demands while achieving high biofuel yields [34,35]. Salt-induced stress has emerged as a promising approach to enhance lipid accumulation in microalgae [22–28]. Under high-salinity conditions, microalgae experience osmotic stress, which alters cellular metabolism and diverts carbon flux toward the synthesis of storage compounds, including lipids. This mechanism enables cells to maintain osmotic balance and survive adverse conditions while simultaneously increasing their lipid content, making salt-induced stress an effective strategy for optimizing biodiesel feedstock [29,30]. Additionally, salt stress influences the fatty acid profile of microalgae, often increasing the proportion of saturated and monounsaturated fatty acids, which are ideal for biodiesel production due to their stability and combustion efficiency [24].

Church et al. [36] demonstrated that increasing salt concentration in synthetic saline wastewater significantly reduced the growth rate of *Chlorella vulgaris* while enhancing its total lipid content and altering its fatty acid profiles. Similarly, Rismeni and Shariati [37]

found that salt stress not only increased lipid content—including omega-3 fatty acids—but also improved cell settling properties, which could benefit downstream processing. Additionally, Li et al. [38] noted that in desert-adapted *Chlorella* sp. TLD6B, an optimal level of salt stress (approximately 0.2 M NaCl) triggered a significant increase in lipid accumulation, supported by transcriptomic evidence of upregulated genes involved in fatty acid and triacylglycerol biosynthesis. Furthermore, two-stage cultivation strategies that combine light and salt stress have been employed to further enhance lipid productivity and stimulate the synthesis of additional high-value metabolites such as carotenoids and antioxidants in CVU. Finally, Pandit et al. [39] highlighted that the effects of salinity are multifaceted, impacting not only biomass yield but also the composition of fatty acids—critical factors for biodiesel quality.

While these studies provide valuable insights into the impact of salt stress on algal growth and lipid accumulation, our work advances the field by integrating salt-induced stress with thermal pretreatment and utilizing anaerobic digestate effluent (ADE) as a nutrient source. This innovative combination aims to enhance biodiesel and biogas production while offering a sustainable solution by maximizing the value of waste streams.

This study evaluates the bioenergy potential of CSO and CVU cultivated in anaerobic digestate effluent (ADE) through a combined approach of stress induction and thermal pretreatment. While salt-induced stress and heat pretreatment have individually demonstrated their efficacy in enhancing lipid accumulation, their combined effects remain underexplored. To address this gap, this research evaluates the synergistic effects of salt-induced stress and heat pretreatment on lipid biosynthesis and methane yield, offering insights into optimizing biofuel production. Specifically, this paper presents findings on (1) the effects of salt stress induction as a stressor to promote lipid storage in both species, (2) the differential impact of ADE concentrations on biochemical composition (lipids, proteins, and carbohydrates) across species, and (3) the influence of various thermal pretreatment conditions on BMP. By analyzing biomass composition, fatty acid methyl ester (FAME) profiles, and biogas yields alongside energy balance assessments, this research underscores the effectiveness of integrating stress and pretreatment strategies. The results reveal significant species-specific responses, particularly in terms of lipid and methane yield optimization, emphasizing the necessity of tailored strategies for maximizing biofuel outputs depending on the target biofuel type and *Chlorella* species.

2. Materials and Methods

2.1. Experimental Design

This study assessed the bioenergy potential of CSO and CVU using ADE as a nutrient source under varying cultivation and stress conditions. This study represents a continuation of earlier studies [40] that established the feasibility of using ADE as a low-cost nutrient medium for microalgae cultivation. Here, we extend that work by incorporating salt-induced stress and thermal pretreatment to further enhance lipid accumulation and optimize methane production, thereby integrating dual biofuel production from a single feedstock. Based on those findings, we selected a lower ADE concentration (3% v/v) to minimize ammonia toxicity and a higher concentration (5% v/v) to provide a richer nutrient environment. Furthermore, the 5% ADE was split into two conditions—with and without the addition of 0.2 M NaCl on Day 8—to assess the effects of salt-induced stress on lipid accumulation and overall biomass composition. Although this design does not constitute a full factorial optimization framework, it enabled us to assess the relative impacts of these parameters on bioenergy production. Future work will employ a factorial design and response surface methodology to model the interactions between variables and to predict optimal conditions that maximize methane yield while minimizing energy input.

Microalgae were grown in a 50 L photobioreactor under four conditions: BG-11 (control), 3% ADE, 5% ADE without stress (ADE5_nostress), and 5% ADE with salt-induced stress (ADE5_stress, 0.2 M NaCl added on Day 8). The photobioreactor maintained controlled conditions (25 °C, 7000 lux, 16:8 h light/dark cycle, CO₂ supplementation at 85 mL/min). Pre-cultured inoculum (10% *v/v*, initial density $\sim 4.5 \times 10^6$ cells/mL) was prepared in BG-11 medium, while ADE was collected, diluted, and analyzed for nutrient composition to mitigate ammonia toxicity. Biochemical analyses quantified proteins, carbohydrates, and lipids. Lipid profiling using gas chromatography provided fatty acid methyl ester (FAME) composition for biodiesel quality assessment.

The biochemical methane potential (BMP) of harvested biomass was tested via anaerobic digestion, with thermal pretreatment (40 °C or 90 °C for 4 or 10 h) applied only to ADE5_stress (where the highest lipid content observed) to evaluate its effect on methane yields. Energy efficiency was calculated as the ratio of methane energy output to the thermal pretreatment energy input, ensuring an optimal energy balance. This design investigated the effects of ADE as a nutrient medium, salinity stress on biomass composition, and thermal pretreatment for optimizing bioenergy production, with statistical analyses (ANOVA, Fisher's LSD test, $p < 0.05$) used to identify significant species-specific responses.

2.2. Microalgae Strains and Pre-Cultivation Condition

CSO and CVU were used in the study. CSO was isolated from anaerobic digestate effluent (ADE) of a 1MW electrical production capacity biogas plant, BIOGAS LAGADA S.A. (Kolchiko-Lagadas, Thessaloniki, Greece), and identified morphologically using a Zeiss Axio Imager Z2 microscope (Carl Zeiss, Oberkochen, Germany). Genetic identification, based on PCR amplification and sequencing of 18S rRNA and *rbcL* genes, confirmed its close relation to CSO with 99% identity via GenBank database comparison (GenBank No. KU948991). The CVU strain was obtained from the MicroAlgae Culture Collection (TAU-MAC). Both strains were maintained in BG-11 medium, containing nutrients in the following concentrations: (g/L) NaNO₃ (1.5), K₂HPO₄·3H₂O (0.04), MgSO₄·7H₂O (0.075), CaCl₂·2H₂O (0.036), citric acid (0.006), ammonium ferric citrate (0.006), Na₂EDTA (0.001), and Na₂CO₃ (0.02); and (mg/L) H₃BO₃ (2.86), MnCl₂·4H₂O (1.81), ZnCl₂ (0.222), Na₂MoO₄·2H₂O (0.391), CoCl₂·6H₂O (0.05), and CuSO₄·5H₂O (0.079). All reagents used were of analytical grade and purchased from Sigma-Aldrich (St. Louis, MO, USA). All nutrient solutions and glassware were autoclaved at 121 °C for 20 min (Witeg, WAC-P60, Wertheim, Germany) to ensure sterility during the early growth stages. Methods were performed as described by Psachoulia et al. [40].

2.3. Microalgae Cultivation in a Photobioreactor

2.3.1. Photobioreactor (PBR) Setup and Operation

A 50 L tubular photobioreactor (PBR) was designed and constructed from Schott glass tubes (Schott AG, Mainz, Germany) for microalgae cultivation under artificial lighting. The system comprises eight straight tubes, each 1.4 m in length and 61 mm in internal diameter, interconnected by seven J-bend joints. The total illuminated surface area was optimized to ensure uniform light distribution to the culture medium, with illumination provided by cool white LED strips (6000 K, 11 W/m, i-WL LED, Germany) delivering 7000 lux under a 16:8 h light/dark photoperiod. Circulation within the PBR is achieved using a Blau Reef Motion 8KDC pump (Blau Aquaristic, Barcelona, Spain), which provides a maximum flow rate of 8000 L/h and ensures efficient mixing, maintaining turbulent flow conditions ($Re > 3000$) for optimal light penetration and nutrient distribution. Carbon dioxide was supplied at a controlled rate of 85 mL/min to support microalgal growth, providing inorganic carbon and keeping pH below 8.5. The reactor is equipped with

online monitoring sensors for pH, dissolved oxygen (DO), and temperature, connected to a programmable logic controller (PLC) and a data logger. Temperature was maintained constant at 25 °C throughout the experiments by an air-conditioner and an aquarium heater of 50 W (Aquael Neoheater 50 W). Prior to experiments, the reactor was sterilized with 12% NaClO (technical grade). The system's modularity, glass construction, and compact design provide durability, ease of sterilization, and optimal conditions for high biomass productivity in controlled laboratory settings.

2.3.2. Inoculum Preparation

Prior to photobioreactor inoculation, algae strains were cultured in Erlenmeyer flasks (170 mL BG-11 medium, initial $OD_{600nm} \approx 0.35$) under controlled conditions. The cultures were grown in a shaking incubator (GFL 3031, GFL Gesellschaft für Labortechnik mbH, Burgwedel, Germany) at 110 rpm and 25 °C, with a continuous supply of atmospheric air at 250 mL/min, passed through 0.2 µm filters. Additionally, 2.5 mL/min of CO₂ was supplied using precision flowmeters (FL-3845G-HVR, Omega Engineering, Norwalk, CT, USA). Cool white LED strips (6000 K, 11 W/m) provided 1200 lux illumination, measured using a portable light meter (SP 200K, Sauter, Kern & Sohn, Balingen, Germany), on a 16 h light/8 h dark cycle. After 18 days, biomass was harvested by centrifugation at $5000 \times g$ for 10 min and subsequently was used to inoculate the photobioreactor (10% *v/v* inoculum, achieving an initial cell density of $\sim 4.5 \times 10^6$ cells/mL) [40].

2.3.3. Nutrient Media Preparation and Composition

Approximately 30 L of ADE was collected in a plastic tank from the output stream of a 1 MW electricity production biogas plant (BIOGAS LAGADA S.A., Kolchiko-Lagadas, Greece) processing livestock waste. Samples were transported to the laboratory and immediately centrifuged ($5000 \times g$, 10 min) using an Eppendorf 5810R refrigerated centrifuge (Eppendorf Austria GmbH, Wien, Austria), and filtered (Whatman Inc., 150 mm diameter, Grade 1, 11 µm pore size). Nutrient concentrations (N-NH₄, N-NO₃, TN, P-PO₄, and COD) were determined using standard HACH cuvette tests-kits and a UV-V spectrophotometer (DR 3900, HACH, Loveland, CO, USA). Digestate elemental analysis was performed via an Agilent 7850 ICP-MS, an Inductively Coupled Plasma Mass Spectrometer (Agilent Technologies, Santa Clara, CA, USA). To mitigate ammonia nitrogen inhibition, ADE was diluted to 3% and 5% (*v/v*) with distilled water, as recommended by Collos and Harrison [41]. BG-11 medium was prepared as a control, and the nutrient compositions of the media are summarized in Table 1.

Following the presentation of the physicochemical properties of the ADE batches and their respective dilutions in Table 1, it is important to clarify the management of the collected digestate and the nutrient replenishment strategy employed throughout the experiments. A total volume of 30 L of ADE was collected for each experimental round and subsequently divided into three 10 L portions, each serving as a replicate for the preparation of the culture media. These 10 L portions were utilized to establish the initial 3% and 5% ADE concentrations within the 50 L photobioreactor. Prior to experimentation, preliminary data from a collaborative project, partially published in this issue [42], guided our nutrient management approach. For the 3% ADE cultures, an average total nitrogen (N) consumption rate of 4.74 mg/L/day was anticipated, while for 5% ADE, a rate of 9.13 mg/L/day was expected. To maintain adequate nitrogen levels, we implemented a replenishment strategy, adding approximately 60.45 mL of raw ADE every four days to the 3% ADE cultures and 116.5 mL to the 5% ADE cultures. Phosphorus (P) was also carefully managed, with initial additions of KH₂PO₄ to achieve target P-PO₄ concentrations of 12.1 mg/L (0.605 g total P added) for 3% ADE and 15.6 mg/L (0.78 g total P added) for 5%

ADE. Subsequent P additions were made every 2 days for 3% ADE and every 3–4 days for 5% ADE cultures, respectively, based on observed consumption rates of 1.11 mg/L/day and 1.3 mg/L/day. This ensured that neither N nor P became limiting factors. The implemented strategy confirms that the 10 L ADE portions provided ample volume for initial medium preparation, and the nutrient replenishment for each replicate throughout the experimental period until Day 8, where salt was added to the culture medium.

Table 1. Nutrient media composition.

Composition (mg/L)	ADE	3% ADE	5% ADE	BG-11
N-NH ₄	3536 ± 36	107 ± 1.08	175.4 ± 1.8	n.d. ¹
N-NO ₃	92 ± 8.1	2.77 ± 0.24	4.6 ± 0.41	247.84
TN	3920 ± 66	117.6 ± 1.98	195 ± 3.3	247.84
P	81.4 ± 5.8	2.1 ± 0.17	4.2 ± 0.29	5.50
Organic N	292 ± 21.9	7.83 ± 0.68	15 ± 1.1	n.d.
COD	24,200 ± 153	726 ± 4.59	1210 ± 7.65	n.d.
Ca	369 ± 3.1	11.07 ± 0.09	18.45 ± 0.16	9.81
Fe	54 ± 1.4	1.62 ± 0.04	2.71 ± 0.07	1.28
Mg	225 ± 5.3	6.75 ± 0.16	11.25 ± 0.27	6.98
Mn	6.33 ± 0.35	0.19 ± 0.01	0.32 ± 0.02	0.50
Na	1884.6 ± 4.5	56.54 ± 0.14	94.23 ± 0.23	212.28
Cl	1633.6 ± 5.9	49.01 ± 0.18	81.68 ± 0.3	18.02
K	3161 ± 2.7	94.83 ± 0.08	158.05 ± 0.14	13.70
Cu	2 ± 0.03	0.06 ± 0.00	0.10 ± 0.00	0.02
EC	49.7 dS/m	2.17 dS/m	3.15 dS/m	n.a. ²
pH	8.3	8.0	8.1	7.1

¹ n.d. = not detected, ² n.a. = not available.

2.3.4. Salt Stress Treatment

Salt stress was induced in CVU and CSO cultures grown in 5% ADE to enhance lipid accumulation. On the 8th day of cultivation, sodium chloride (NaCl; Sigma-Aldrich, St. Louis, MO, USA) was added to the cultures to reach a final concentration of 0.2 M (11.7 g/L), a level shown to promote lipid biosynthesis while maintaining cell viability [43–46]. The concentration of 0.2 M NaCl was selected based on previous studies that demonstrated its effectiveness in triggering lipid accumulation without causing excessive cell lysis or inhibiting growth. A pre-dissolved NaCl solution was uniformly mixed into the medium, and electrical conductivity (EC) was measured using a portable conductivity meter (HACH HQ40d) to confirm the target value of approximately 20 dS/m. Therefore, to raise the EC of 1 L of 5% ADE (3.15 dS/m) to 20 dS/m, 10.78 g of NaCl were diluted into the medium to induce the stress to initialize the lipid accumulation in the *Chlorella* species.

2.3.5. Biomass Harvesting

The microalgal biomass was harvested from the photobioreactor using a 0.4 µm ultrafiltration membrane (Kubota), which was immersed in a 5 L PMMA tank connected downstream to the reactor system via a bypass pipeline. A peristaltic pump (Shenghen LabV1, Shenghen pump yz1515x) was employed to draw the culture liquid through the membrane. As the liquid passed through the membrane pores, the biomass was separated from the medium and retained within the membrane vessel, effectively increasing its concentration in the 5 L PMMA tank. The concentrated biomass was collected directly from the membrane container via a discharge outlet located at the base of the tank, eliminating the need for scraping and ensuring a non-invasive and efficient collection process. The slurry was drained directly into collection containers. Subsequently, the harvested biomass

was centrifuged at $5000\times g$ for 10 min, filtered (Whatman Inc., Sanford, ME, USA, 150 mm pore size), and stored at $-20\text{ }^{\circ}\text{C}$ for further analysis.

2.4. Thermal Pretreatment

To evaluate the effect of heat pretreatment on enhancing BMP, CSO, and CVU, under “ADE5_stress”, cultivation conditions, the harvested samples were subjected to different temperature–time combinations at $40\text{ }^{\circ}\text{C}$ and $90\text{ }^{\circ}\text{C}$ with exposure durations of 4 and 10 h for each temperature. Heating was conducted in a shaking water bath (OLS-26, Grant Instruments Ltd., Royston, UK), in 1000 ml Erlenmeyer flasks. The thermal pretreatment conditions of $40\text{ }^{\circ}\text{C}$ and $90\text{ }^{\circ}\text{C}$ for durations of 4 and 10 h were chosen because $40\text{ }^{\circ}\text{C}$ reflects mesophilic conditions favorable for enzymatic activity during digestion, while $90\text{ }^{\circ}\text{C}$ represents a commonly used threshold for effective cell wall [36]. After pretreatment, the biomass was cooled to room temperature and stored at $4\text{ }^{\circ}\text{C}$ until further use [25,47]. Additionally, untreated control treatments for both CSO and CVU were performed at $25\text{ }^{\circ}\text{C}$ under ADE5 conditions with salt stress. These control values were used to normalize both datasets for conducting the ANOVA.

2.5. Biomass Composition Analysis

2.5.1. Protein Determination

Protein content was extracted from 2 mg of freeze-dried biomass using 9.6 mL of 0.5 M NaOH solution containing 5% methanol (*v/v*) and 0.4 mL of 0.05 M phosphate buffer [48]. The mixture was subjected to sonication in an ice bath for 10 min at 50% of the sonicator’s maximum amplitude to ensure cell lysis and protein release. An additional 5 mL of NaOH solution (0.5 M, 5% *v/v* MeOH) was added, and the sample was heated to $100\text{ }^{\circ}\text{C}$ for 30 min under continuous stirring. Protein content was quantified using a Micro-BCA kit (Thermo Scientific, Waltham, MA, USA) and a microplate spectrophotometer (Mindray MR-96A, microplate reader, Mindray Medical International Ltd., Shenzhen, China). A calibration curve was generated using Bovine Serum Albumin (BSA) as the standard.

2.5.2. Carbohydrate Determination

2 mg of lyophilized algal biomass was treated with 1 mL of 2.5 M HCl and incubated at $100\text{ }^{\circ}\text{C}$ for 3 h under continuous stirring to hydrolyze polysaccharides, oligosaccharides, and disaccharides into monosaccharides. The hydrolyzed solution was neutralized with 2.5 M NaOH and centrifuged. Carbohydrate content was measured using the phenol-sulfuric acid method, where samples were treated with 1 mL of 1% (*w/v*) phenol solution and 5 mL of 96% (*w/w*) sulfuric acid. Absorbance was measured at 483 nm (Lamda 35, Perkin Elmer, Akron, OH, USA) [49]. A D-glucose calibration curve was used to calculate carbohydrate concentration, expressed as glucose equivalents.

2.5.3. Lipid Determination

Lipid content was quantified using the Bligh and Dyer extraction method [50]. Lyophilized algal biomass (5 mg) was treated with a solvent mixture of methanol, chloroform, and distilled water (2:1:0.8 *v/v*). The suspension was sonicated in an ice bath for 20 min at 50% amplitude (Vibra Cell VC-505, Sonics & Materials, Newtown, CT, USA). After centrifugation, the solvent was collected. The extraction was repeated three times to maximize lipid recovery. Subsequently, 3 mL chloroform, 3 mL methanol, and 2.7 mL distilled water (2:2:1.8 *v/v*) were added to the solvent phase. The lower phase, containing lipids, was separated, dried at $45\text{ }^{\circ}\text{C}$ overnight, and weighed using a precision microbalance (XP 105, Mettler Toledo, Greifensee, Switzerland) to determine the total lipid content.

2.5.4. Fatty Acid Profile Analysis

Fatty acid contents were determined by gas chromatography (GC-FID) using a Shimadzu GC-2010 Plus High-End Gas Chromatograph (Shimadzu Europa GmbH, Duisburg, Germany) equipped with a Flame Ionization Detector (FID) after lipid extraction by the Soxhlet procedure [51]. The extracted fatty acids were trans-esterified in a methanolic potassium hydroxide solution, and the FAME samples were analyzed. A Supelco SP2560 column (100 m × 0.25 mm × 0.20 µm; Merck KGaA, Darmstadt, Germany) was used for separation. Helium (grade 99.999%) was employed as the carrier gas at a flow rate of 2 mL/min. The injection volume was 1 µL with a split ratio of 1:20, and the injector and detector temperatures were set at 250 °C. The temperature program was as follows: initial oven temperature at 110 °C (7 min), increasing at 3 °C/min to 190 °C (2 min), followed by a first step at 0.5 °C/min to 205 °C, a second at 5 °C/min to 230 °C (5 min), and a final step at 5 °C/min to 240 °C, held for 5 min. The total run time was 82.67 min. Results were identified using GC solution software by comparing certified reference material's (CRM47885, Supelco® 37 Component FAME Mix, Sigma-Aldrich) retention time peaks with the r.t. peaks of samples. Fatty acid values, including SFA, MUFA, and PUFA, were expressed as weight percentages (% of total FAs).

2.5.5. Volatile Solids (VS) Analysis

Initially, the sample was dried and weighed in a pre-dried and pre-weighed dish. The dish with the sample was then ignited in a muffle furnace at 550 °C for 4 h. After ignition, the dish was cooled in a desiccator to room temperature and weighed again. The difference in weight before and after ignition represented the volatile solids content. This method was based on the Fixed and Volatile Solids Ignited at 550 °C protocol according to APHA 2540-E [52].

2.6. Biochemical Methane Potential (BMP) Test

The biochemical methane potential was determined using a Bioprocess Gas Endeavour AMPTS® III system (S/N: 1100-2100-5100-1235; BPC Instruments (Haining) Co., Ltd., Haining, China) following Bioprocess Control protocols. The system consisted of fifteen 500 mL Duran Schott bottles (400 mL working volume, 100 mL headspace) submerged in a thermostatic water bath. Biogas production was measured volumetrically via a water displacement method using a graduated cylinder connected to the bottle headspace via a gas outlet. Teflon caps sealed each bottle. Our BMP experiments, conducted over 30 days, revealed that the largest incremental increase in biogas production occurred between days 15 and 25, with methane yields stabilizing by approximately Day 25.

The substrate quantity added to each bottle was calculated using the following equation:

$$m_i = ISR \times \frac{m_{tot} \times VS_s}{VS_i + 2 \times VS_s}$$

where:

- m_i : Mass of inoculum (g);
- m_{tot} : Total mass in the bottle (400 g);
- VS_s : Volatile solids in the substrate;
- VS_i : Volatile solids in the inoculum;
- ISR : Inoculum-to-substrate ratio, defined as:

$$ISR = \frac{\text{quantity of inoculum } VS}{\text{quantity of substrate } VS} = 2$$

This ratio followed the guidelines provided by the manufacturer [53].

Bioreactors containing both inoculum and substrate (samples) and inoculum only (blanks) were purged with nitrogen gas for 2 min to establish anaerobic conditions. The bioreactors were then incubated in a thermostatic water bath at a mesophilic temperature (40 °C) for 30 days. Biogas production was monitored daily.

Biochemical methane potential (*BMP*) is defined as the volume of methane produced per unit amount of organic substrate material added to the reactor and can be expressed by the following equation:

$$BMP = \frac{(V_s - V_i)}{m_{VS, SS}}$$

where:

- V_s : Accumulated volume of biomethane from the reactor containing the sample (substrate and inoculum);
- V_i : Volume of biomethane produced by the inoculum present in the sample bottle;
- $m_{VS, SS}$: Amount of organic material (substrate) contained in the sample bottle.

This equation quantifies the efficiency of methane production from the added organic substrate material under the given experimental conditions.

2.7. Energy Output (kJ) Based on the Biogas Production Potential

The energy output (EE) was calculated using the formula:

$$E \text{ (kJ)} = BMP \text{ (L CH}_4\text{/g VS)} \times VS \text{ (g)} \times \text{Methane Energy Content (kJ/L)}$$

Values for *BMP* and *VS* were derived from experimental data, while methane energy content was taken as 35.8 kJ/L.

2.8. Energy Efficiency

Energy efficiency (%) was calculated by dividing methane energy output (E_{CH_4}) by pretreatment energy input ($E_{\text{pretreatment}}$), then multiplying by 100, reflecting the balance between produced energy and energy consumed, using the following formulas.

$$\text{Energy Efficiency(\%)} = \frac{E_{CH_4}}{E_{\text{pretreatment}}} \times 100$$

where E_{CH_4} : Energy output from methane production, calculated as:

$$E_{CH_4} = BMP \text{ (L CH}_4\text{/g VS)} \times VS \text{ (g)} \times \text{Methane Energy Content (kJ/L)}$$

Energy input (pretreatment):

$E_{\text{pretreatment}}$: Energy input for heating the biomass suspension, calculated as:

$$E_{\text{pretreatment}} = \rho \times Cp \times (T_{\text{target}} - T_{\text{ambient}}) \times V$$

where ρ is the density of the suspension (1 kg/L), Cp is the specific heat capacity of water (4.18 kJ/kg °C), T_{target} is the pretreatment temperature, T_{ambient} is the ambient temperature (25 °C), and V is the biomass volume (L). This calculation quantifies the balance between methane energy output and pretreatment energy input [54].

Energy Output

Energy Output (kJ) was calculated based on the biogas production potential

The energy output (EE) was calculated using the formula:

$$E \text{ (kJ)} = BMP \text{ (L CH}_4\text{/g VS)} \times VS \text{ (g)} \times \text{Methane Energy Content (kJ/L)}$$

Values for *BMP* and *VS* were derived from experimental data, while methane energy content was taken as 35.8 kJ/L.

2.9. Statistical Analysis

To ensure the robustness and reliability of our findings, all experiments were conducted with three independent biological replicates ($n = 3$). This involved dividing the initial 30 L of digestate into three equal portions (10 L each) and using each portion to establish a separate culture for each treatment condition. Each experiment was then performed three times using these independently established cultures. Descriptive statistics, including mean, median, standard deviation, and relative standard deviation, were calculated using Minitab v22 and MS Excel. ANOVA was employed to assess the effects of treatments, species, and cultivation conditions on the measured parameters. Prior to ANOVA, the assumptions of normality and homogeneity of variances were rigorously verified using the Shapiro–Wilk test and Levene’s test, respectively. Fisher’s least significant difference (LSD) test was subsequently used to identify significant differences ($p < 0.05$) among group means. Significant differences identified by the LSD test are denoted by distinct letters within tables and figures. This post-hoc test was selected due to its sensitivity in detecting treatment effects without overly conservative adjustments for multiple comparisons, aligning with its established use in similar microalgal studies [55]. Furthermore, Z-normalization was applied to standardize the data across different experiments. This technique minimizes variability stemming from extraneous factors and enhances the detection of genuine biological signals. Although commonly employed in high-throughput analyses like RNA-seq and microarray studies, the principles of Z-normalization are equally valid for improving comparative accuracy in studies such as ours [56,57].

3. Results and Discussion

3.1. Biochemical Composition of Microalgae Under Different Cultivation Conditions

3.1.1. Protein Accumulation

Analyzing protein content in CVU and CSO cultivated in BG11, ADE3 (3% anaerobic digestate effluent), ADE5_stress (5% ADE with stress), and ADE5_nostress reveals distinct accumulation patterns influenced by species and environmental factors (Table 2, Figure 1a,b). Under the nutrient-replete medium BG-11, protein content was notably high, with CSO achieving 35.67% and CVU slightly higher at 39.40%, reflecting inherent differences in protein synthesis capacity, with CSO possibly adapted to utilizing organic nitrogen from digestate [58]. In ADE3, CSO exhibited an increase in protein content (39.80%) compared to BG11, reflecting enhanced nitrogen assimilation efficiency from ADE. In contrast, CVU protein content decreased slightly to 35.33% compared to BG11, suggesting species-specific differences in nitrogen utilization from ADE’s complex nutrient profile. This indicates that ADE’s nutrient composition may stimulate protein synthesis more effectively in CSO, possibly due to its better adaptation to organic nitrogen utilization [59]. In ADE5_nostress, protein content decreased for both species compared to BG11, with CVU at 29.70% and CSO at 28.83%. This reduction indicates potential inhibitory effects at higher ADE concentrations, such as ammonia toxicity or nutrient imbalances. These findings highlight the limitations of nutrient assimilation in both species under non-stressed ADE5 conditions, suggesting that the nutrient profile of ADE5 may not sufficiently support optimal protein synthesis at higher concentrations. Under ADE5_stress, both species experienced significant protein reduction (CVU to 13.00%, CSO to 31.63%), attributed to stress-induced redirection of resources towards lipid accumulation, a survival strategy under nitrogen starvation [60–62]. However, CSO maintained higher protein content, suggesting greater stress resilience.

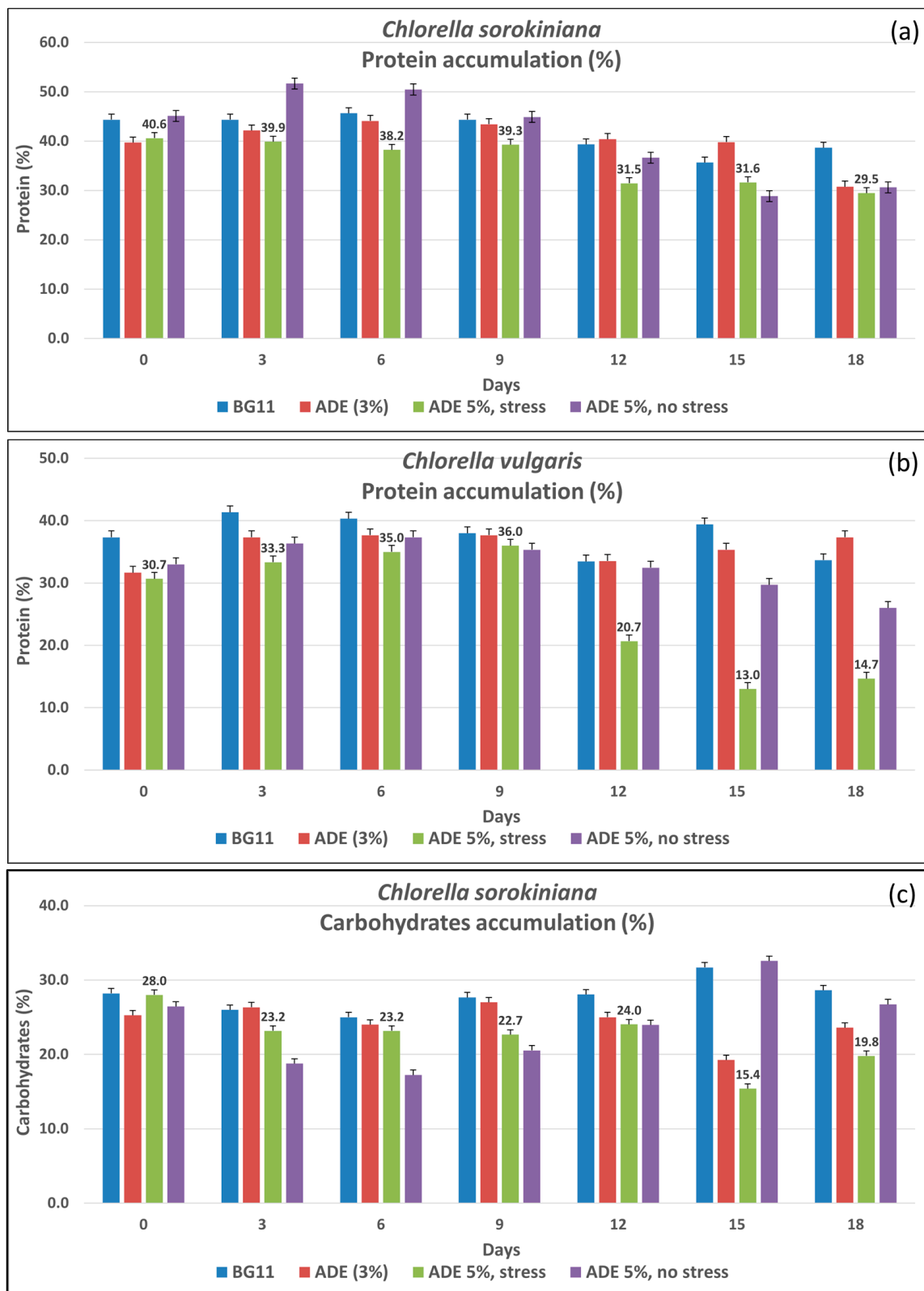


Figure 1. Cont.

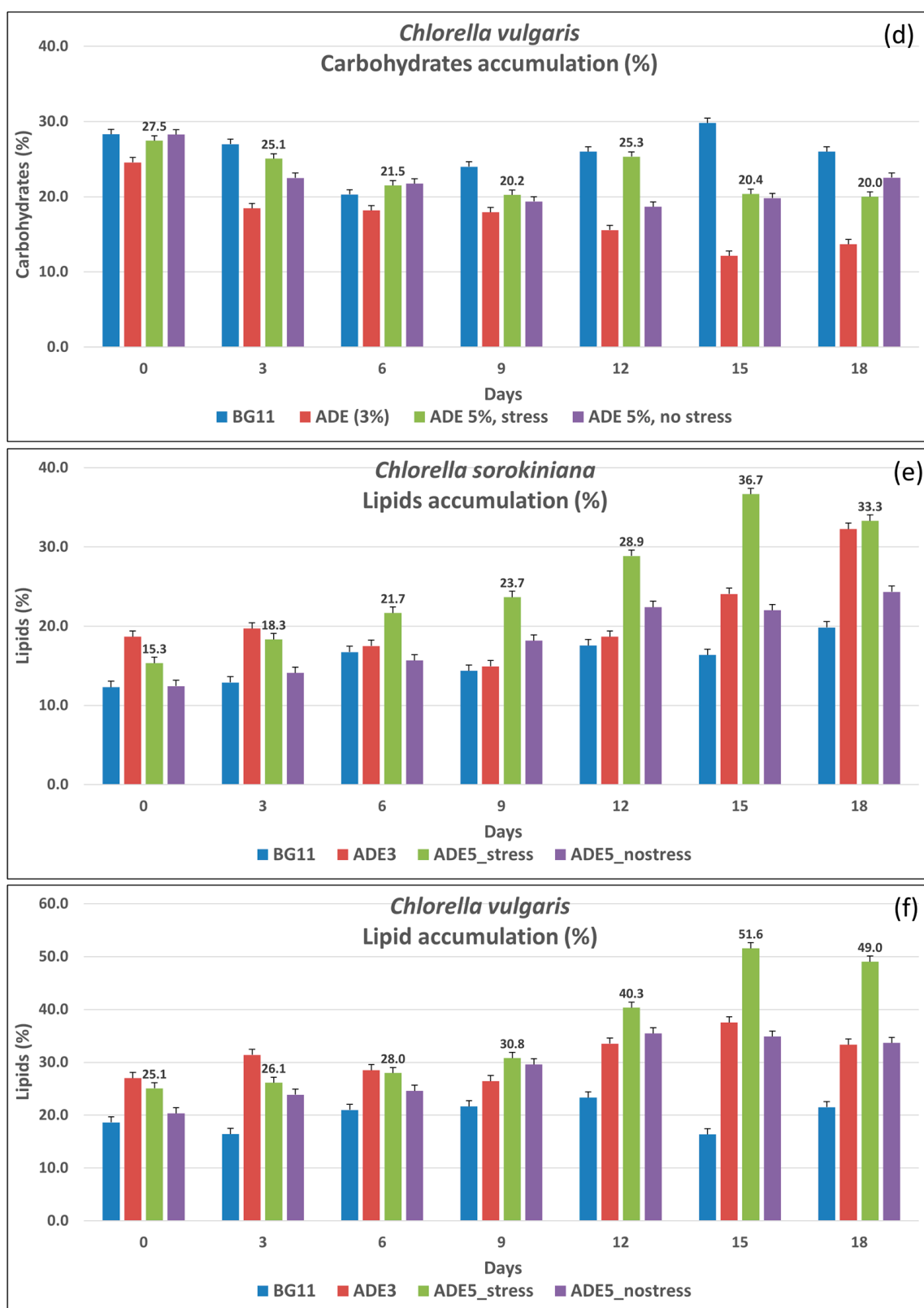


Figure 1. Protein accumulation (%) in (a) *C. sorokiniana* and (b) *C. vulgaris*, carbohydrates accumulation (%) in (c) *C. sorokiniana* and (d) *C. vulgaris*, lipids accumulation (%) in (e) *C. sorokiniana*, and (f) *C. vulgaris* cultivated in different media (BG11, ADE3, ADE5_stress, ADE5_nostress) over 18 days. Error bars represent standard error of triplicate measurements.

Table 2. Mean values of proteins, carbohydrates, and lipid content of *Chlorella sorokiniana* and *Chlorella vulgaris* under different cultivation conditions.

Cultivation Conditions	Proteins (%)	Carbohydrates (%)	Lipids (%)
CSO BG11	35.67 ± 4.0 ¹ ab ²	31.70 ± 8.3 a	16.37 ± 1.8 e
CSO ADE3	39.80 ± 3.6 a	19.25 ± 1.0 b	24.07 ± 1.6 d
CSO ADE5_stress	31.63 ± 1.4 bc	15.40 ± 0.7 bc	36.67 ± 1.1 bc
CSO ADE5_nostress	28.83 ± 1.2 c	32.57 ± 0.5 a	22.00 ± 0.7 d
CVU BG11	39.40 ± 1.0 a	29.82 ± 2.5 a	16.37 ± 1.8 e
CVU ADE3	35.33 ± 1.3 ab	12.13 ± 1.8 c	37.53 ± 0.4 b
CVU ADE5_stress	13.00 ± 1.0 d	20.37 ± 5.5 b	51.57 ± 1.4 a
CVU ADE5_nostress	29.70 ± 4.3 bc	19.81 ± 5.5 b	34.87 ± 0.7 c
Mean	31.67	22.63	29.93
LSD ³	6.00	6.27	2.08

¹ Standard deviation ($n = 3$). ² Mean values with significant differences indicated by distinct letters ($p < 0.05$) according to LSD test. ³ LSD = least significant differences value at ($p < 0.05$).

3.1.2. Carbohydrates Accumulation

Analyzing carbohydrate content in CVU and CSO cultivated in BG11, ADE3 (3% anaerobic digestate effluent), ADE5_stress (5% ADE with stress), and ADE5_nostress (5% ADE without stress) reveal distinct accumulation patterns influenced by species-specific metabolism and environment (Table 2, Figure 1c,d). These variations reflect the balance between carbon allocation for carbohydrate storage, lipid biosynthesis, and protein synthesis, modulated by nutrient availability and stress. In BG11, CSO exhibited higher carbohydrate content (31.7%) than CVU (29.82%), suggesting inherent metabolic variations, potentially prioritizing carbohydrate storage under nutrient-rich conditions [63]. CVU carbohydrate content decreased (12.13%) compared to CSO (19.25%), suggesting differential ADE nutrient utilization, possibly due to varied organic carbon assimilation efficiency or inhibitory compounds [64,65]. In ADE5_nostress, CSO carbohydrate content increased significantly to 32.57% compared to BG11 (31.70%), indicating that higher ADE concentrations without stress favor carbohydrate accumulation in CSO due to increased organic carbon availability [66,67]. However, for CVU, carbohydrate content in ADE5_nostress (19.81%) remained lower than in BG11 (29.82%), reflecting species-specific differences in response to ADE conditions. Under ADE5_stress, CVU carbohydrate content decreased (20.37%), potentially prioritizing lipid accumulation under stress [68–71], while CSO remained relatively stable (15.40%), possibly demonstrating stress resilience [63].

3.1.3. Lipids Accumulation

Analyzing lipid production in CVU and CSO cultivated in BG11, ADE3 (3% anaerobic digestate effluent), ADE5_stress (5% ADE with stress), and ADE5_nostress reveals a complex interplay between species-specific metabolism and environmental factors (Table 2, Figure 1e,f). In BG11, both species showed similar lipid contents (16.37%), suggesting comparable lipid biosynthesis capacities under optimal nutrient conditions [72].

However, in ADE3, CVU exhibited a marked increase in lipid content (37.53%), compared to BG11 (16.37%), demonstrating ADE's stimulatory effect on lipid biosynthesis, likely due to its rich organic carbon and nutrient profile [73,74]. CSO also showed increased lipid content in ADE3 (24.07%), but less pronounced than CVU, possibly due to inherent metabolic differences and adaptations to nutrient environments. Increasing ADE concentration to 5% without stress (ADE5_nostress) slightly decreased lipid content in CVU (34.87%), suggesting potential inhibitory effects of higher ADE concentrations in the absence of stress [64], possibly due to accumulated inhibitory compounds or a suboptimal nutrient balance. In contrast, CSO in ADE5_nostress accumulated 22.00% lipids, still lower than

CVU. Under ADE5_stress, CVU lipid content increased dramatically (51.57%), highlighting stress-induced effects such as salt stress redirect metabolic flux towards lipid accumulation as a survival mechanism [70,72]. CSO showed a moderate increase under stress (36.67%), significantly lower than CVU, potentially reflecting a different stress response or adaptation to the ADE environment [63,65], possibly prioritizing other survival mechanisms [75]. This study demonstrates that salt-induced stress significantly enhances lipid accumulation in *C. vulgaris* (CVU) by up to 51.57%, a level that outperforms many alternative methods reported in the literature. For example, nitrogen starvation, a widely studied stressor, typically increases lipid content in *Chlorella* species by 30–45%. These observations align with literature highlighting nitrogen starvation as a key trigger for lipid accumulation [70,72] while acknowledging species-specific tolerances and adaptations to stress [75].

The increased lipid accumulation observed in *Chlorella vulgaris* (CVU) under salt stress is mainly due to metabolic adjustments triggered by osmotic and oxidative stresses. These adjustments enhance the biosynthesis and accumulation of lipids, particularly triacylglycerols (TAGs). High salinity creates an osmotic imbalance, causing algal cells to redirect their metabolic pathways toward lipid production, which serves as protective energy reserves and helps maintain cell integrity under stress. Under osmotic stress, CVU reallocates carbon to lipid synthesis to uphold cellular integrity and functionality. Salinity has been shown to trigger specific metabolic pathways linked to fatty acid biosynthesis, resulting in elevated levels of triacylglycerols, which act as energy storage compounds vital for cell survival under stress conditions. Furthermore, transcriptomic analyses of salt-stressed *Chlorella* sp. have revealed the upregulation of genes involved in lipid biosynthesis pathways, such as acetyl-CoA carboxylase (ACCase), ketoacyl-ACP synthase II (KAS II), and glycerol-3-phosphate dehydrogenase (GPDH), which play a direct role in triacylglycerol (TAG) synthesis [38,39].

Studies supporting these findings have shown a significant increase in saturated and monounsaturated fatty acids under elevated salinity conditions, indicating a shift toward more stable lipid molecules suitable for biofuel production [76]. Specifically, Pandit et al. [39] reported increased production of palmitic and oleic acids under higher salinity, both essential components for biodiesel.

Therefore, the lipid accumulation under salt stress observed in CVU is a survival adaptation mechanism, optimizing its metabolism for cellular protection and energy storage.

3.1.4. Impact of Media and Stress on Biochemical Profiles of *Chlorella*

The composition of cultivation media plays a pivotal role in shaping the biochemical profiles of CSO and CVU, with distinct impacts on protein, carbohydrate, and lipid accumulation. These differences directly influence the suitability of biomass for bioenergy production. Nutrient-rich conditions in BG-11 favored protein and carbohydrate synthesis, supporting growth-oriented metabolic pathways, as observed in previous studies by Yadav et al. [77], Morowvat and Ghasemi [78], Dahiya et al. [79], and Singh et al. [80]. Furthermore, the low lipid levels observed in both species (16.37%) align with the findings of Vishwakarma et al. [81], who reported that BG-11 medium supports high carbohydrate and protein production in *Chlorella* species while limiting lipid accumulation due to its nutrient-replete nature. In contrast, ADE3 stimulated moderate lipid accumulation while maintaining high protein levels, showcasing its potential as a nutrient source for balancing the growth and storage of macromolecules. In this study, ADE3 supported a protein content of 39.80% in CSO and 35.33% in CVU, alongside moderate lipid accumulation (CSO: 24.07%, CVU: 37.53%), emphasizing its suitability as a balanced nutrient medium. These findings align with Zhang et al. [82], who found that using diluted anaerobically digested kitchen waste facilitated optimal biomass production in *Chlorella sorokiniana*, with lipid

accumulation ranging from 30.27% to 41.69%, highlighting the nutrient-balancing effect of ADE. In ADE5 without stress, CSO exhibited the highest carbohydrate content (32.57%), highlighting its efficient carbon allocation toward carbohydrate storage in the absence of stress. This aligns with findings by Magdaong et al. [83] and Chai et al. [84], who reported stable carbohydrate content and enhanced carbohydrate storage in *C. sorokiniana* under non-stress and nutrient-rich conditions. Zhu et al. [85] further observed increased starch accumulation in *C. sorokiniana* with glucose supplementation under favorable conditions, while Dahiya et al. [79] and Cecchin et al. [86] linked efficient carbohydrate storage to upregulated carbon flux pathways in non-stress environments. These findings support the results of this study, positioning *C. sorokiniana* as a strong candidate for carbohydrate-rich biomass applications, such as bioethanol production. Under salinity stress (ADE5 with stress), lipid biosynthesis became the dominant metabolic pathway, with CVU achieving 51.57% lipid content, surpassing CSO at 36.67%. This metabolic shift reflects a redirection of resources from growth-oriented macromolecules to energy storage, positioning CVU as a strong candidate for lipid-based bioenergy applications. These findings align with previous studies demonstrating the role of salinity stress in enhancing lipid biosynthesis. Zhang et al. [87] reported a 2.16-fold increase in lipid productivity in *C. sorokiniana* under salinity stress due to carbon redistribution from starch to lipids, while El-Adl et al. [88] observed increased lipid accumulation supported by elevated proline levels for stress tolerance. Similarly, Yun et al. [89] found lipid content in *C. vulgaris* increased from 12.7% to 24.5% under salinity stress, and Li et al. [90] identified upregulated fatty acid biosynthesis genes under stress conditions. The superior lipid accumulation in CVU observed here underscores its potential for biofuel applications, validating salinity stress as an effective strategy to optimize lipid yields in microalgae.

These findings underscore the importance of tailoring cultivation strategies to media-specific factors, such as nutrient availability, ADE concentration, and stress induction, to optimize biomass composition for bioenergy yields. ADE's organic carbon content and nutrient profile, combined with stress-inducing conditions, create an ideal environment for enhancing lipid productivity, especially in CVU. Additionally, species-specific adaptations to nutrient and stress conditions, such as CSO's resilience in maintaining protein and carbohydrate levels, highlight the potential for integrating different *Chlorella* strains into bioenergy systems to meet diverse production goals.

3.2. Fatty Acid Methyl Ester (FAME) Profiles

Analyzing the fatty acid methyl ester (FAME) profiles of CSO and CVU (Figure 2) cultivated in 5% anaerobic digestate effluent (ADE5) without induced stress reveals insights into their lipid composition and biodiesel production potential. FAME analysis reveals variations in fatty acid profiles reflecting the influence of the growth medium on fatty acid biosynthesis, which impacts biodiesel quality.

CVU exhibited significantly higher polyunsaturated fatty acid (PUFA) content (31.7%) compared to CSO (15.4%), while CSO had a higher monounsaturated fatty acid (MUFA) level (40.6%) and saturated fatty acid (SFA) content (31.6%) relative to CVU (33.7% MUFA and 20.4% SFA). These differences underscore species-specific metabolic adaptations, with CSO's higher MUFA and SFA content contributing to superior fuel stability, improved combustion properties, and lower freezing points—key attributes for biodiesel quality. In contrast, CVU's elevated PUFA levels suggest applications requiring enhanced oxidative balance, though they may reduce fuel stability. Among individual fatty acids, CSO showed significantly higher palmitic acid (C16:0, 29.1%) and oleic acid (C18:1, 33.5%) levels, both essential for biodiesel stability and performance. Conversely, CVU demonstrated greater proportions of linoleic acid (C18:2, 19.1%) and linolenic acid (C18:3, 12.7%), which

enhanced its PUFA dominance. Stearic acid (C18:0) levels were slightly higher in CVU (2.5%) compared to CSO (1.9%), and CVU also contained a greater diversity of minor fatty acids (1.3%) compared to CSO (0.6%). These differences suggest ADE5 influences fatty acid biosynthesis pathways, likely due to its complex nutrient environment compared to standard media [91].

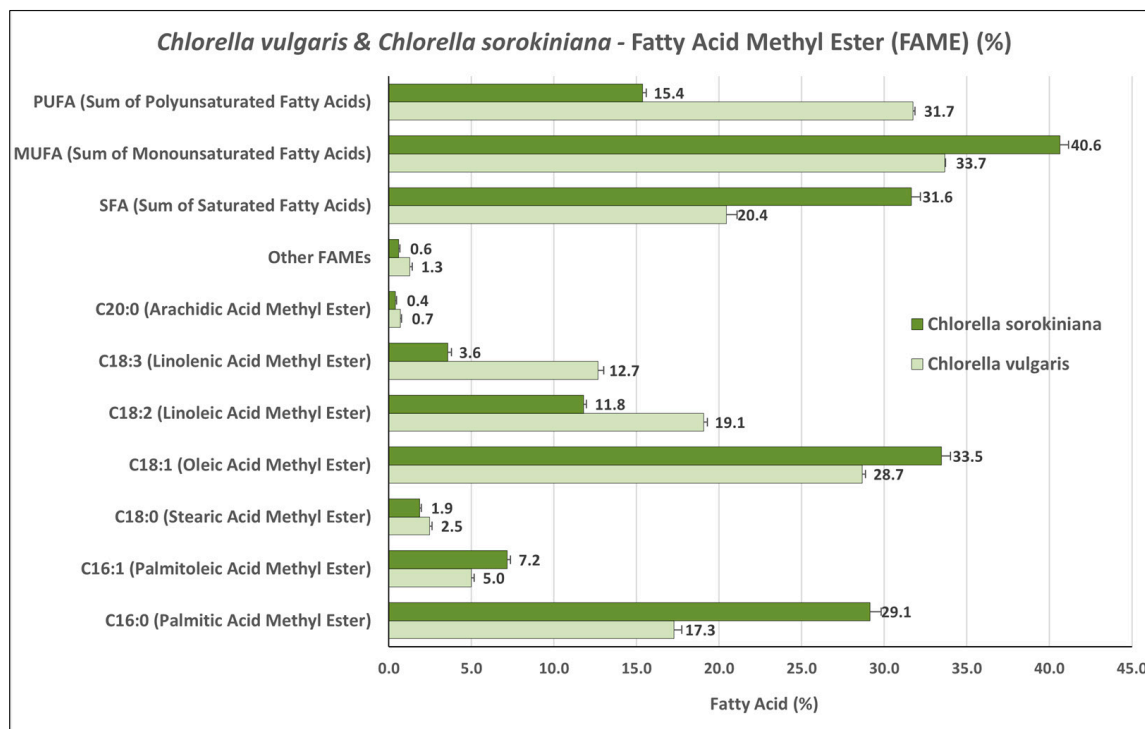


Figure 2. Fatty Acid Methyl Esters (FAMES) profile of *C. vulgaris* and *C. sorokiniana* cultivated in 5% ADE. Values represent the percentage composition of each fatty acid methyl ester. Error bars represent the standard error of triplicate measurements.

The higher SFA content in CSO might enhance membrane stability or energy storage, while higher PUFAs in CVU could relate to membrane fluidity or stress response [92]. Comparing these findings with studies on other *Chlorella* species grown under different conditions [93,94] highlights variations in FAME profiles, emphasizing the influence of cultivation conditions (e.g., heterotrophic vs. photoautotrophic) and species-specific metabolism on fatty acid biosynthesis [61,93]. The observed FAME profiles impact biodiesel properties. Higher SFAs in CSO suggest increased biodiesel stability but potentially higher viscosity and cloud point. Higher PUFAs in CVU could improve cold flow but compromise oxidative stability, possibly necessitating antioxidants. The higher oleic acid in CSO benefits both stability and cold flow. Further analysis is needed to determine if the biodiesel produced meets standards like EN 14214 or ASTM D6751 [95]. Optimizing FAME composition could involve exploring different extraction methods [96], manipulating growth conditions [61,93], and potentially genetic modification. Further research into the mechanisms by which ADE5 influences fatty acid biosynthesis, including gene expression analysis and nutrient component impact, and exploring interactions within the ADE5 microbial community, would enable tailored lipid composition for optimal biodiesel production.

3.3. BMP: Influence of Anaerobic Digestate Effluent and Stress

Analyzing the biochemical methane potential (BMP) of CVU and CSO cultivated in different media—BG11 (control), ADE3 (3% anaerobic digestate effluent), ADE5_stress (5% ADE with stress), and ADE5_no stress (5% ADE without stress)—reveals distinct

patterns influenced by species, nutrient availability, and stress responses (Table 3). BMP, a key indicator of bioenergy potential, reflects the interplay between biomass biochemical composition (carbohydrate, protein, and lipid content) and anaerobic digestion efficiency.

Table 3. Biogas production (mL(biogas)/gVS) of *Chlorella sorokiniana* and *Chlorella vulgaris* under different cultivation conditions.

Cultivation Conditions	mL(biogas)/gVS
CSO BG11	407.1 ± 2.0 c ¹
CSO ADE3	399.3 ± 3.4 d
CSO ADE5_stress	418.3 ± 3.9 b
CSO ADE5_nostress	407.9 ± 5.1 c
CVU BG11	414.5 ± 1.4 b
CVU ADE3	408.1 ± 0.6 c
CVU ADE5_stress	432.8 ± 2.4 a
CVU ADE5_nostress	409.2 ± 1.2 c
Means	412.1
LSD ²	4.8

¹ Means values ($n = 3$) with significant differences indicated by distinct letters ($p < 0.05$) according to LSD test.

² LSD = least significant differences value at ($p < 0.05$).

In BG11, CVU showed a slightly higher BMP (414.5 mL CH₄/g VS) than CSO (407.1 mL CH₄/g VS), suggesting similar methane production potential under optimal conditions, potentially due to subtle differences in biochemical composition impacting biodegradability. This aligns with previous research on species' biogas potential, with methane yields ranging from 140 to 360 dm³/kg VS [97]. In ADE3, both species exhibited a decrease in BMP (CVU at 408.1 mL CH₄/g VS and CSO at 399.3 mL CH₄/g VS) compared to BG11, suggesting that even low ADE concentrations might introduce inhibitory compounds or negatively alter biomass composition, potentially through ammonia or heavy metal inhibition [98], or changes in substrate degradability due to the shift from defined to complex organic media. The decrease in BMP for CSO in ADE3 (399.3 mL CH₄/g VS) is primarily due to a significant reduction in carbohydrate content (19.25%), which limits the availability of readily degradable substrates for methane production. Additionally, the increase in protein content (39.80%) can lead to ammonia inhibition during anaerobic digestion, further impacting BMP. Limited nutrient availability and potential inhibitory effects of ammonia in ADE3 also contribute to this decline. A stark contrast emerged under ADE5_stress: CVU BMP increased substantially to 432.80 mL CH₄/g VS (highest among all treatments), while CSO BMP increased to 418.3 mL CH₄/g VS. This species-specific stress response highlights its impact on bioenergy potential. The BMP increase under ADE5_nostress (407.9 mL CH₄/g VS) can be attributed to the recovery of carbohydrate content to 32.57%, which enhances methane yield, and a decrease in protein content to 28.83%, reducing the risk of ammonia inhibition. Furthermore, the balanced nutrient profile in ADE5 supports favorable biomass composition and improves digestion efficiency, resulting in BMP levels closer to the BG11 control. The increased BMP in stressed CVU could be due to stress-induced lipid accumulation [60,99], enhancing methane yield, whereas CSO may prioritize different survival mechanisms over lipid accumulation under stress. In ADE5_no stress, both CVU (409.2 mL CH₄/g VS) and CSO (407.90 mL CH₄/g VS) maintained BMPs similar to BG11, indicating that higher ADE concentration without stress does not significantly affect bioenergy potential. The slight decrease in CVU might be due to potential inhibitor accumulation or less favorable composition at higher ADE concentrations, while CSO appears less sensitive to higher ADE without stress [40]. These species-specific BMP differences under varying ADE conditions and stress could stem from

distinct genetic backgrounds influencing biochemical composition, varying metabolic stress responses (particularly lipid accumulation under salt stress), ADE composition (inhibitory compounds and nutrient availability), and microalgae-microbial community interactions in ADE impacting anaerobic digestion [100,101].

3.4. Impact of Thermal Pretreatment and Energy Efficiency of Thermal Pretreatment for Enhanced Methane Production

Figure 3a,b present the biochemical methane potential (BMP) of CSO and CVU under varying thermal pretreatment conditions and an untreated control, measured over 30 days. For CSO, the results demonstrate that milder thermal pretreatment at 40 °C for 10 h (40_10) achieved the highest BMP (472 mL CH₄/g VS), surpassing treatments at 90 °C. This emphasizes that prolonged exposure to lower temperatures enhances biomass digestibility more effectively than shorter treatments at higher temperatures, possibly due to sustained enzymatic activity and gradual cell wall disruption. In contrast, for CVU higher temperatures combined with longer durations (e.g., 90_10) significantly increased BMP to 481 mL CH₄/g VS, indicating greater cell wall disruption and intracellular substrate release under these conditions. However, pretreatments at 40 °C (40_4 and 40_10) resulted in lower BMP values of 380 and 387 mL CH₄/g VS, respectively, compared to the control (415 mL CH₄/g VS). This could be attributed to the biochemical and structural composition of CVU's cell wall, which may exhibit limited disruption under milder pretreatment conditions. Unlike CSO, which shows enhanced enzymatic activity and gradual cell wall breakdown at lower temperatures, CVU may require higher thermal severity to achieve effective cell wall disruption and intracellular substrate release. Both species displayed increased BMP during the initial days of the process, with gradual stabilization observed toward the end, indicating similar digestion patterns despite differences in the effects of pretreatment.

Thermal pretreatment significantly influences both biochemical methane potential (BMP) and the energy efficiency of anaerobic digestion using biomass using the ADE5 medium. Table 4 presents BMP and energy efficiency data under cultivation conditions ADE5_stress for CSO and CVU subjected to different thermal pretreatment conditions (40_4, 40_10, 90_4, and 90_10), compared to the untreated control. For CSO, BMP generally increased with increasing temperature and pretreatment time. Pretreatment at 40 °C (40_4) resulted in a BMP of 407 mL CH₄/g VS, similar to the control (407 mL CH₄/g VS). Extending the pretreatment time to 10 h (40_10) significantly enhanced BMP to 472 mL CH₄/g VS, indicating that longer exposure to mild heat can improve biomass digestibility. At 90 °C, the 4-hour treatment (90_4) yielded 425 mL CH₄/g VS, and a longer duration of 10 h (90_10) further increased BMP to 448 mL CH₄/g VS. This suggests that higher temperatures promote more effective cell wall disruption and release of intracellular substrates, although the magnitude of BMP enhancement might plateau with extended pretreatment durations. The superior energy efficiency observed for CSO at 40 °C (2.67%) highlights the potential of this low-energy approach, offering an optimized balance between methane yield and energy input. These findings underscore the species-specific benefits of tailoring thermal pretreatment parameters, particularly considering the energy savings and the substantial improvement in BMP at milder conditions for CSO. CVU exhibited a different response pattern. Pretreatments at 40 °C (40_4 and 40_10) resulted in BMP values of 380 and 387 mL CH₄/g VS, respectively, showing less BMP improvement compared to CSO and less than control (415 mL CH₄/g VS). However, 90 °C pretreatments significantly enhanced methane production, reaching 474 mL CH₄/g VS (90_4) and 481 mL CH₄/g VS (90_10), indicating greater cell disruption and release of intracellular substrates. Similar to CSO, energy efficiency decreased as the severity of pretreatment for CVU increased. While 40_4 had the highest energy efficiency (2.54%), likely due to low energy input, the 90_10 pretreatment showed the lowest energy efficiency (0.55%). This demonstrates the trade-off

between higher BMP and reduced energy efficiency under severe pretreatment conditions. For example, while 90 °C for 10 h (90_10) maximized BMP for CVU (481 mL CH₄/g VS), it resulted in the lowest energy efficiency (0.55%), highlighting the significant energy cost of severe thermal treatments. Conversely, milder pretreatment conditions (e.g., 40 °C for 4 h) achieved the highest energy efficiency (2.54%) for CVU but at the cost of lower BMP (380 mL CH₄/g VS). A similar pattern is observed for CSO, where the highest BMP (472 mL CH₄/g VS) at 40_10 involved a moderate energy efficiency trade-off (1.24%), compared to the highest energy efficiency (2.67%) under 40_4. This aligns with literature suggesting that algal species display diverse susceptibilities to thermal pretreatment, influencing their methane production potential and energy requirements for cell disruption [102,103]. The biochemical composition of each species and its alteration due to pretreatment also plays a role in impacting methane yield [104]. The interaction between microalgae and the microbial community during cultivation can further influence biomass digestibility and response to thermal treatment, affecting methane production during AD [105]. Integrating energy efficiency analysis alongside BMP assessment is crucial for selecting sustainable biogas production strategies. This combined approach considers the economic and environmental viability of microalgae-based biogas production by evaluating both methane yield and the energy balance of the process. The observed trade-offs between BMP and energy efficiency across different species and pretreatments suggest that a balanced approach is essential for maximizing bioenergy production from microalgae. Further research on characterizing the structural and biochemical changes due to thermal treatment, and their influence on microbial communities during AD [98], is crucial for optimizing pretreatment conditions that maximize both methane output and energy efficiency. By considering both the potential methane yield and energy efficiency of different thermal pretreatments, we can develop more sustainable and cost-effective biogas production strategies.

Table 4. Methane production and Energy Efficiency of CSO and CVU of ADE5 under different thermal pretreatment conditions.

Cultivation Conditions	BMP (mL biogas/gVS)	Energy Input (kJ)	Energy Output (kJ)	Energy Efficiency (%)
CSO 40_4	407 ± 6.5 e ¹	250.8	14,570.6	2.67 ± 0.003 a ²
CSO 40_10	472 ± 2.5 b	627.0	16,897.6	1.24 ± 0.005 c
CSO 90_4	425 ± 1.5 d	1085.0	15,215.0	0.93 ± 0.003 f
CSO 90_10	448 ± 2.1 c	2712.5	16,038.4	0.49 ± 0.002 h
CVU 40_4	380 ± 3.2 f	250.8	13,604.0	2.54 ± 0.017 b
CVU 40_10	387 ± 3.1 f	627.0	13,848.6	1.01 ± 0.007 e
CVU 90_4	474 ± 3.6 b	1085.0	16,969.2	1.03 ± 0.006 d
CVU 90_10	481 ± 8.0 a	2712.5	17,219.8	0.55 ± 0.002 g
Control_25 °C- ³	380 ± 1.9 f	-	-	- ⁵
Means	434			1.31
LSD ⁴	-			0.01

¹ Mean values (*n* = 3) with significant differences indicated by distinct letters (*p* < 0.05) according to LSD after Z-normalization. ² Means values with significant differences indicated by distinct letters (*p* < 0.05) according to LSD. ³ Untreated control presented as mean of both CSO & CVU, ADE5 with salt stress cultivated for both species at 25 °C, and used for normalizing the datasets for the ANOVA. ⁴ LSD = least significant differences value at (*p* < 0.05). ⁵ Energy efficiency cannot be calculated since 25 °C is used in the energy input formula (Section 2.8) as the ambient temperature.

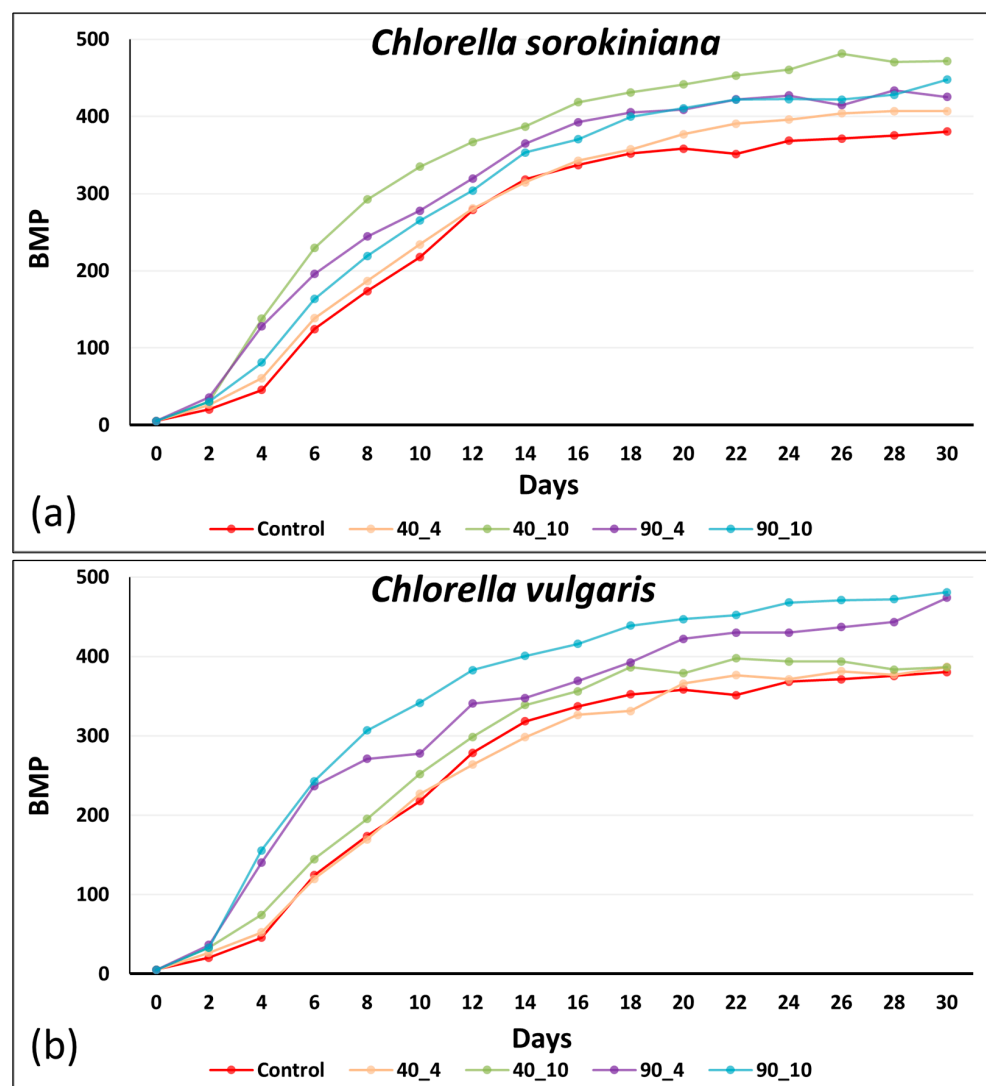


Figure 3. Cumulative biogas yield over 30 days for ADE5 with salt stress in (a) *sorokiniana* and (b) *vulgaris*. Control and thermal pretreatments at 40 °C and 90 °C for 4 and 10 h.

3.5. Economic Feasibility and Scalability of Implementation in Industrial Biofuel Production Plans

The combined use of salt-induced stress and thermal pretreatment optimizes biofuel outputs from cultivating species, significantly enhancing lipid accumulation and methane yields. Based on our laboratory-scale BMP assays, which show that maximum methane production is achieved by Day 25, we propose that an optimal hydraulic retention time (HRT) of approximately 25 days would balance complete digestion with minimized energy input and operational downtime, thereby enhancing the overall economic viability of a full-scale biogas production plant. Economically, the approach capitalizes on cost-effective substrates such as ADE, reducing dependency on synthetic nutrients and integrating waste valorization into the production process including waste heat from the cogeneration of heat and power units (CHP) in typical biogas plants. This aligns with circular economy principles, contributing to sustainability. However, scalability challenges arise in maintaining consistent stress conditions and achieving energy-efficient thermal pretreatment. While thermal pretreatment at higher temperatures boosts methane yields, energy inputs may offset gains if not optimized. The energy efficiency of milder treatments demonstrates potential but requires balancing against biofuel outputs. Industrial adoption would benefit from modular photobioreactor designs and tailored stress and pretreatment protocols suited for specific strains like CVU or CSO. Species-specific lipid and biodiesel profiles

further necessitate targeted strategies to meet industrial quality standards. Investments in pilot-scale testing, energy modeling, and integration with existing wastewater facilities will determine economic viability. This method offers a scalable framework for industrial biofuel systems with advancements in pretreatment technologies and energy efficiency optimization. Lifecycle assessments are needed to comprehensively evaluate economic and environmental impacts, considering factors such as land use, water footprint, and greenhouse gas emissions. Ultimately, market demand for both biodiesel and biogas will strongly influence the economic feasibility of large-scale implementation.

3.6. Economic Viability Analysis

Energy Input vs. Output: For CSO at 40 °C for 4 h, the thermal pretreatment requires an energy input of 250.8 kJ, which costs approximately EUR 0.020 (using the EU average price of EUR 0.2889/kWh, where 1 kWh = 3600 kJ). The corresponding methane energy output is 14,570.6 kJ, valued at about EUR 1.168. This results in a net energy profit of approximately EUR 1.148 per batch, with an energy efficiency of 2.67%. For CVU at 90 °C for 10 h, the energy input rises to 2712.5 kJ (costing roughly EUR 0.217), while the output is 17,219.8 kJ (valued at about EUR 1.381). This yields a net profit of approximately EUR 1.164 per batch despite a lower energy efficiency of 0.55%.

Cost–Benefit Comparison: The milder condition (40 °C for 4 h) for CSO provides a high net energy profit with minimal energy expenditure, making it economically favorable—especially at small scales. Although the 90 °C, 10 h treatment for CVU slightly increases the net profit per batch, it requires approximately 10.8 times more energy input, which would elevate operational costs if scaled up.

Benchmarking Against Literature: Our figures are in line with those reported by Wang et al. [25], who noted that milder pretreatment conditions (40–60 °C) are more energy-efficient, and by Mendez et al. [27], who observed that 90 °C pretreatments incur higher operational costs. For instance, Wang et al. reported net profits in the range of EUR 1.00–EUR 1.20 per batch, which is comparable to our findings (EUR 1.148–EUR 1.164).

Scalability and Key Cost Drivers: Scaling to industrial volumes (e.g., 1000 L batches) is expected to reduce the energy cost per unit due to economies of scale. For example, scaling CSO at 40 °C for 4 h could lower energy input costs to around EUR 20 per batch versus EUR 217 for the CVU 90 °C, 10 h condition. Thermal energy consumption (which accounts for approximately 90% of pretreatment costs) and the use of ADE as a low-cost nutrient source (reducing substrate costs by 30–40% compared to synthetic media) are the main cost drivers.

The analysis confirms that the process is economically viable, particularly under milder conditions (40 °C for 4 h), which offers a favorable balance between energy efficiency (2.67%) and net energy profit (EUR 1.148 per batch) (Table 5). It is important to note that these economic metrics are based on current EU energy prices (EUR 0.2889/kWh) and laboratory-scale data. As the process is scaled up, economies of scale and further process optimizations are expected to enhance both energy efficiency and net profit margins.

Table 5. Economic metrics per batch in Euros.

Cultivation Conditions	Energy Input (EUR)	Energy Output (EUR)	Net Profit (EUR)
CSO, 40 °C, 4 h	EUR 0.020	EUR 1.168	EUR 1.148
CSO, 90 °C, 10 h	EUR 0.217	EUR 1.381	EUR 1.164
CVU, 40 °C, 4 h	EUR 0.020	EUR 1.168	EUR 1.148
CVU, 90 °C, 10 h	EUR 0.217	EUR 1.381	EUR 1.164

(Energy cost in the EU in 2024 is EUR 0.2889/kWh; 1 kWh = 3600 kJ; Eurostat 2024).

4. Conclusions

This study demonstrates that integrating salt-induced stress with thermal pretreatment significantly enhances the bioenergy potential of *Chlorella* species cultivated in anaerobic digestate effluent. Our results reveal that salt stress—applied at an optimal concentration of 0.2 M NaCl—induces a marked increase in lipid accumulation, while subsequent thermal pretreatment further improves methane yields during anaerobic digestion. Notably, milder thermal pretreatment conditions (40 °C for 4 h) achieve a superior balance between methane yield and energy efficiency (2.67% for CSO and 2.54% for CVU) compared to harsher conditions, which, although yielding slightly higher methane production, incur significantly greater energy inputs.

The economic viability analysis reinforces these findings: under optimal conditions, the net energy profit per batch is approximately EUR 1.15, with minimal energy expenditure. This favorable cost–benefit balance is further enhanced using anaerobic digestate effluent as a nutrient medium, which reduces cultivation costs by 30–40% relative to synthetic media and promotes waste valorization in line with circular economy principles.

While our current study adopts a comparative design to evaluate discrete conditions, future work will benefit from a full factorial optimization framework and response surface methodology to systematically refine process parameters and develop predictive models for both biodiesel and biogas outputs. Such studies will further enhance our understanding of the trade-offs between methane yield and energy input, ultimately supporting the scaling up of this integrated bioenergy production process.

In summary, our integrated approach—combining salt-induced stress, thermal pretreatment, and cost-effective nutrient sourcing—offers a promising pathway for sustainable bioenergy production from microalgae. These findings provide a solid foundation for scaling up the process, and further pilot-scale investigations will be critical for validating its industrial applicability.

Author Contributions: Conceptualization, T.S.; methodology, T.S. and P.S.; software, T.S., P.S. and T.K.; validation, T.S. and S.G.; formal analysis, T.S. and S.G.; investigation, T.S., S.G. and P.S.; resources, T.S.; data curation, T.S. and S.G.; writing—original draft preparation, T.S. and S.G.; writing—review and editing, T.S., S.G., P.F., P.S. and T.K.; visualization, T.S. and S.G.; supervision, T.S., T.K. and P.S.; project administration, T.S.; funding acquisition, T.S. All authors have read and agreed to the published version of the manuscript.

Funding: This research was co-funded by the European Union’s Horizon Europe Innovation Action HORIZON-CL5-2022-D3-02 (Sustainable, secure and competitive energy supply), under the “Accelerating the sustainable production of advanced biofuels and RFNBOs—from feedstock to end-use” (FUELPHORIA) project (Grant Agreement No. 101118286). Views and opinions expressed are however those of the author(s) only and do not necessarily reflect those of the European Union or CINEA. Neither the European Union nor CINEA can be held responsible for them.

Data Availability Statement: The data presented in this study are available, upon request, from the corresponding author.

Acknowledgments: The authors wish to acknowledge operational manager Apostolos Polychrous of Biogas Lagada S.A. for the industrial tests and the provision of appropriate quantities of digestate. The authors also wish to acknowledge all staff members of Qlab P.C. for their individual roles that contributed to the implementation of this study, thank you Vassiliki Tsioni, and Panagiotis Pantazis.

Conflicts of Interest: Themistoklis Sfetsas and Sopio Ghoghoberidze were employed by Qlab Private Company. They declare that the research was conducted in the absence of any commercial or financial relationships that could be construed as a potential conflict of interest.

References

- Mendez, L.; Mahdy, A.; Ballesteros, M.; González-Fernández, C. Methane Production of Thermally Pretreated *Chlorella vulgaris* and *Scenedesmus* sp. Biomass at Increasing Biomass Loads. *Appl. Energy* **2014**, *129*, 238–242. [\[CrossRef\]](#)
- Mendez, L.; Mahdy, A.; Ballesteros, M.; González-Fernández, C. Biomethane Production Using Fresh and Thermally Pretreated *Chlorella vulgaris* Biomass: A Comparison of Batch and Semi-Continuous Feeding Mode. *Ecol. Eng.* **2015**, *84*, 273–277. [\[CrossRef\]](#)
- Rahman, Q.M.; Zhang, B.; Wang, L.; Shahbazi, A. A Combined Pretreatment, Fermentation and Ethanol-Assisted Liquefaction Process for Production of Biofuel from *Chlorella* sp. *Fuel* **2019**, *257*, 116026. [\[CrossRef\]](#)
- Das, P.K.; Rani, J.; Rawat, S.; Kumar, S. Microalgal Co-Cultivation for Biofuel Production and Bioremediation: Current Status and Benefits. *BioEnergy Res.* **2022**, *15*, 1–26. [\[CrossRef\]](#)
- Hajinajaf, N.; Mehrabadi, A.; Tavakoli, O. Practical Strategies to Improve Harvestable Biomass Energy Yield in Microalgal Culture: A Review. *Biomass Bioenergy* **2021**, *145*, 105941. [\[CrossRef\]](#)
- Bahrim, R.Z.K.; Wazir, N.A.; Jaapar, A.S.; Abidin, Q.H.Z.; Wahab, N.F.A.; Khairulanwar, M.K.M.; Jalil, M.M.; Bakri, F.A.M.; Harom, Z.; Nor, M.G.M.; et al. Advancing Renewable Energy Through Open Tanks Microalgae Cultivation for Biofuel Production: Opportunities, Challenges, and Innovative Solutions. In Proceedings of the International Petroleum Technology Conference, Dhahran, Saudi Arabia, 12 February 2024; p. IPTC-24530-EA.
- Siddiki, S.Y.A.; Mofijur, M.; Kumar, P.S.; Ahmed, S.F.; Inayat, A.; Kusumo, F.; Badruddin, I.A.; Khan, T.M.Y.; Nghiem, L.D.; Ong, H.C.; et al. Microalgae Biomass as a Sustainable Source for Biofuel, Biochemical and Biobased Value-Added Products: An Integrated Biorefinery Concept. *Fuel* **2022**, *307*, 121782. [\[CrossRef\]](#)
- Falfushynska, H. Advancements and Prospects in Algal Biofuel Production: A Comprehensive Review. *Phycology* **2024**, *4*, 548–575. [\[CrossRef\]](#)
- Alazaiza, M.Y.D.; Albahnasawi, A.; Al Maskari, T.; Abujazar, M.S.S.; Bashir, M.J.K.; Nassani, D.E.; Abu Amr, S.S. Biofuel Production Using Cultivated Algae: Technologies, Economics, and Its Environmental Impacts. *Energies* **2023**, *16*, 1316. [\[CrossRef\]](#)
- Muhammad, G.; Alam, M.A.; Mofijur, M.; Jahirul, M.I.; Lv, Y.; Xiong, W.; Ong, H.C.; Xu, J. Modern Developmental Aspects in the Field of Economical Harvesting and Biodiesel Production from Microalgae Biomass. *Renew. Sustain. Energy Rev.* **2021**, *135*, 110209. [\[CrossRef\]](#)
- Zhang, S.; Hou, Y.; Liu, Z.; Ji, X.; Wu, D.; Wang, W.; Zhang, D.; Wang, W.; Chen, S.; Chen, F. Electro-Fenton Based Technique to Enhance Cell Harvest and Lipid Extraction from Microalgae. *Energies* **2020**, *13*, 3813. [\[CrossRef\]](#)
- Lee, S.Y.; Khoiroh, I.; Vo, D.-V.N.; Senthil Kumar, P.; Show, P.L. Techniques of Lipid Extraction from Microalgae for Biofuel Production: A Review. *Environ. Chem. Lett.* **2021**, *19*, 231–251. [\[CrossRef\]](#)
- Marsolek, M.D.; Kendall, E.; Thompson, P.L.; Shuman, T.R. Thermal Pretreatment of Algae for Anaerobic Digestion. *Bioresour. Technol.* **2014**, *151*, 373–377. [\[CrossRef\]](#) [\[PubMed\]](#)
- Bohutskiy, P.; Betenbaugh, M.J.; Bouwer, E.J. The Effects of Alternative Pretreatment Strategies on Anaerobic Digestion and Methane Production from Different Algal Strains. *Bioresour. Technol.* **2014**, *155*, 366–372. [\[CrossRef\]](#)
- Giang, T.T.; Lunprom, S.; Liao, Q.; Reungsang, A.; Salakkam, A. Improvement of Hydrogen Production from *Chlorella* sp. Biomass by Acid-Thermal Pretreatment. *PeerJ* **2019**, *7*, e6637. [\[CrossRef\]](#)
- De Oliveira, M.C.; Bassin, I.D.; Cammarota, M.C. Microalgae and Cyanobacteria Biomass Pretreatment Methods: A Comparative Analysis of Chemical and Thermochemical Pretreatment Methods Aimed at Methane Production. *Fermentation* **2022**, *8*, 497. [\[CrossRef\]](#)
- Markou, G.; Ilkiv, B.; Brulé, M.; Antonopoulos, D.; Chakalis, L.; Arapoglou, D.; Chatzipavlidis, I. Methane Production through Anaerobic Digestion of Residual Microalgal Biomass after the Extraction of Valuable Compounds. *Biomass Convers. Biorefinery* **2022**, *12*, 419–426. [\[CrossRef\]](#)
- Da Silva, C.; Astals, S.; Peces, M.; Campos, J.L.; Guerrero, L. Biochemical Methane Potential (BMP) Tests: Reducing Test Time by Early Parameter Estimation. *Waste Manag.* **2018**, *71*, 19–24. [\[CrossRef\]](#)
- Filer, J.; Ding, H.H.; Chang, S. Biochemical Methane Potential (BMP) Assay Method for Anaerobic Digestion Research. *Water* **2019**, *11*, 921. [\[CrossRef\]](#)
- Du, X.; Tao, Y.; Li, H.; Liu, Y.; Feng, K. Synergistic Methane Production from the Anaerobic Co-Digestion of *Spirulina Platensis* with Food Waste and Sewage Sludge at High Solid Concentrations. *Renew. Energy* **2019**, *142*, 55–61. [\[CrossRef\]](#)
- Passos, F.; Hom-Díaz, A.; Blázquez, P.; Vicent, T.; Ferrer, I. Improving Biogas Production from Microalgae by Enzymatic Pretreatment. *Bioresour. Technol.* **2016**, *199*, 347–351. [\[CrossRef\]](#)
- Córdova, O.; Passos, F.; Chamy, R. Enzymatic Pretreatment of Microalgae: Cell Wall Disruption, Biomass Solubilisation and Methane Yield Increase. *Appl. Biochem. Biotechnol.* **2019**, *189*, 787–797. [\[CrossRef\]](#)
- Gonzalez-Fernandez, C.; Barreiro-Vescovo, S.; De Godos, I.; Fernandez, M.; Zouhayr, A.; Ballesteros, M. Biochemical Methane Potential of Microalgae Biomass Using Different Microbial Inocula. *Biotechnol. Biofuels* **2018**, *11*, 184. [\[CrossRef\]](#)
- Cho, S.; Park, S.; Seon, J.; Yu, J.; Lee, T. Evaluation of Thermal, Ultrasonic and Alkali Pretreatments on Mixed-Microalgal Biomass to Enhance Anaerobic Methane Production. *Bioresour. Technol.* **2013**, *143*, 330–336. [\[CrossRef\]](#)

25. Wang, M.; Lee, E.; Dilbeck, M.P.; Liebelt, M.; Zhang, Q.; Ergas, S.J. Thermal Pretreatment of Microalgae for Biomethane Production: Experimental Studies, Kinetics and Energy Analysis. *J. Chem. Technol. Biotechnol.* **2017**, *92*, 399–407. [\[CrossRef\]](#)
26. Almarashi, J.Q.M.; El-Zohary, S.E.; Ellabban, M.A.; Abomohra, A.E.-F. Enhancement of Lipid Production and Energy Recovery from the Green Microalga *Chlorella vulgaris* by Inoculum Pretreatment with Low-Dose Cold Atmospheric Pressure Plasma (CAPP). *Energy Convers. Manag.* **2020**, *204*, 112314. [\[CrossRef\]](#)
27. Mahdy, A.; Mendez, L.; Ballesteros, M.; González-Fernández, C. Autohydrolysis and Alkaline Pretreatment Effect on *Chlorella vulgaris* and *Scenedesmus* sp. Methane Production. *Energy* **2014**, *78*, 48–52. [\[CrossRef\]](#)
28. Mahdy, A.; Ballesteros, M.; González-Fernández, C. Enzymatic Pretreatment of *Chlorella vulgaris* for Biogas Production: Influence of Urban Wastewater as a Sole Nutrient Source on Macromolecular Profile and Biocatalyst Efficiency. *Bioresour. Technol.* **2016**, *199*, 319–325. [\[CrossRef\]](#)
29. Carrillo-Reyes, J.; Barragán-Trinidad, M.; Buitrón, G. Biological Pretreatments of Microalgal Biomass for Gaseous Biofuel Production and the Potential Use of Rumen Microorganisms: A Review. *Algal Res.* **2016**, *18*, 341–351. [\[CrossRef\]](#)
30. Ganesh Saratale, R.; Kumar, G.; Banu, R.; Xia, A.; Periyasamy, S.; Dattatraya Saratale, G. A Critical Review on Anaerobic Digestion of Microalgae and Macroalgae and Co-Digestion of Biomass for Enhanced Methane Generation. *Bioresour. Technol.* **2018**, *262*, 319–332. [\[CrossRef\]](#)
31. Dos Santos Ferreira, J.; De Oliveira, D.; Maldonado, R.R.; Kamimura, E.S.; Furigo, A. Enzymatic Pretreatment and Anaerobic Co-Digestion as a New Technology to High-Methane Production. *Appl. Microbiol. Biotechnol.* **2020**, *104*, 4235–4246. [\[CrossRef\]](#)
32. Wang, P.; Wang, H.; Qiu, Y.; Ren, L.; Jiang, B. Microbial Characteristics in Anaerobic Digestion Process of Food Waste for Methane Production—A Review. *Bioresour. Technol.* **2018**, *248*, 29–36. [\[CrossRef\]](#)
33. Zhen, G.; Lu, X.; Kobayashi, T.; Kumar, G.; Xu, K. Anaerobic Co-Digestion on Improving Methane Production from Mixed Microalgae (*Scenedesmus* sp., *Chlorella* sp.) and Food Waste: Kinetic Modeling and Synergistic Impact Evaluation. *Chem. Eng. J.* **2016**, *299*, 332–341. [\[CrossRef\]](#)
34. Lizzul, A.M.; Hellier, P.; Purton, S.; Baganz, F.; Ladommatos, N.; Campos, L. Combined Remediation and Lipid Production Using *Chlorella Sorokiniana* Grown on Wastewater and Exhaust Gases. *Bioresour. Technol.* **2014**, *151*, 12–18. [\[CrossRef\]](#) [\[PubMed\]](#)
35. Junttila, D.J.; Bautista, M.A.; Monotilla, W. Biomass and Lipid Production of a Local Isolate *Chlorella Sorokiniana* under Mixotrophic Growth Conditions. *Bioresour. Technol.* **2015**, *191*, 395–398. [\[CrossRef\]](#)
36. Church, J.; Hwang, J.-H.; Kim, K.-T.; McLean, R.; Oh, Y.-K.; Nam, B.; Joo, J.C.; Lee, W.H. Effect of Salt Type and Concentration on the Growth and Lipid Content of *Chlorella vulgaris* in Synthetic Saline Wastewater for Biofuel Production. *Bioresour. Technol.* **2017**, *243*, 147–153. [\[CrossRef\]](#)
37. Rismani, S.; Shariati, M. Changes of the Total Lipid and Omega-3 Fatty Acid Contents in Two Microalgae *Dunaliella salina* and *Chlorella vulgaris* Under Salt Stress. *Braz. Arch. Biol. Technol.* **2017**, *60*, e17160555. [\[CrossRef\]](#)
38. Abdellaoui, N.; Kim, M.J.; Choi, T.J. Transcriptome Analysis of Gene Expression in *Chlorella Vulgaris* under Salt Stress. *World J. Microbiol. Biotechnol.* **2019**, *35*, 141. [\[CrossRef\]](#)
39. Pandit, P.R.; Fulekar, M.H.; Karuna, M.S.L. Effect of Salinity Stress on Growth, Lipid Productivity, Fatty Acid Composition, and Biodiesel Properties in *Acutodesmus Obliquus* and *Chlorella vulgaris*. *Environ. Sci. Pollut. Res.* **2017**, *24*, 13437–13451. [\[CrossRef\]](#)
40. Psachoulia, P.; Schortsianiti, S.-N.; Lortou, U.; Gkelis, S.; Chatzidoukas, C.; Samaras, P. Assessment of Nutrients Recovery Capacity and Biomass Growth of Four Microalgae Species in Anaerobic Digestion Effluent. *Water* **2022**, *14*, 221. [\[CrossRef\]](#)
41. Collos, Y.; Harrison, P.J. Acclimation and Toxicity of High Ammonium Concentrations to Unicellular Algae. *Mar. Pollut. Bull.* **2014**, *80*, 8–23. [\[CrossRef\]](#)
42. Psachoulia, P.; Chatzidoukas, C.; Samaras, P. Study of *Chlorella Sorokiniana* Cultivation in an Airlift Tubular Photobioreactor Using Anaerobic Digestate Substrate. *Water* **2024**, *16*, 485. [\[CrossRef\]](#)
43. Li, X.; Yuan, Y.; Cheng, D.; Gao, J.; Kong, L.; Zhao, Q.; Wei, W.; Sun, Y. Exploring Stress Tolerance Mechanism of Evolved Freshwater Strain *Chlorella* Sp. S30 under 30 g/L Salt. *Bioresour. Technol.* **2018**, *250*, 495–504. [\[CrossRef\]](#) [\[PubMed\]](#)
44. Ho, S.-H.; Nakanishi, A.; Kato, Y.; Yamasaki, H.; Chang, J.-S.; Misawa, N.; Hirose, Y.; Minagawa, J.; Hasunuma, T.; Kondo, A. Dynamic Metabolic Profiling Together with Transcription Analysis Reveals Salinity-Induced Starch-to-Lipid Biosynthesis in Alga *Chlamydomonas* Sp. JSC4. *Sci. Rep.* **2017**, *7*, 45471. [\[CrossRef\]](#)
45. Srivastava, G.; Nishchal; Goud, V.V. Salinity Induced Lipid Production in Microalgae and Cluster Analysis (ICCB 16-BR_047). *Bioresour. Technol.* **2017**, *242*, 244–252. [\[CrossRef\]](#)
46. Wang, T.; Ge, H.; Liu, T.; Tian, X.; Wang, Z.; Guo, M.; Chu, J.; Zhuang, Y. Salt Stress Induced Lipid Accumulation in Heterotrophic Culture Cells of *Chlorella Protothecoides*: Mechanisms Based on the Multi-Level Analysis of Oxidative Response, Key Enzyme Activity and Biochemical Alteration. *J. Biotechnol.* **2016**, *228*, 18–27. [\[CrossRef\]](#)
47. Wu, H.; Li, J.; Yang, H.; Liao, Q.; Fu, Q.; Liu, Z. Hydrothermal Treatment of *Chlorella* sp.: Influence on Biochemical Methane Potential, Microbial Function and Biochemical Metabolism. *Bioresour. Technol.* **2019**, *289*, 121746. [\[CrossRef\]](#)
48. Schwenzfeier, A.; Wierenga, P.A.; Gruppen, H. Isolation and Characterization of Soluble Protein from the Green Microalgae *Tetraselmis* sp. *Bioresour. Technol.* **2011**, *102*, 9121–9127. [\[CrossRef\]](#) [\[PubMed\]](#)

49. DuBois, M.; Gilles, K.A.; Hamilton, J.K.; Rebers, P.A.; Smith, F. Colorimetric Method for Determination of Sugars and Related Substances. *Anal. Chem.* **1956**, *28*, 350–356. [\[CrossRef\]](#)
50. Bligh, E.G.; Dyer, W.J. A Rapid Method of Total Lipid Extraction and Purification. *Can. J. Biochem. Physiol.* **1959**, *37*, 911–917. [\[CrossRef\]](#)
51. Guihéneuf, F.; Schmid, M.; Stengel, D.B. Lipids and Fatty Acids in Algae: Extraction, Fractionation into Lipid Classes, and Analysis by Gas Chromatography Coupled with Flame Ionization Detector (GC-FID). In *Natural Products from Marine Algae*; Stengel, D.B., Connan, S., Eds.; Methods in Molecular Biology; Springer: New York, NY, USA, 2015; Volume 1308, pp. 173–190. ISBN 978-1-4939-2683-1.
52. Standard Methods Committee of the American Public Health Association; American Water Works Association; Water Environment Federation. 2540 Solids. In *Standard Methods for the Examination of Water and Wastewater*; Lipps, W.C., Baxter, T.E., Braun-Howland, E., Eds.; APHA Press: Washington, DC, USA, 2023.
53. Weik, M.H. *Computer Science and Communications Dictionary*; Springer US: Boston, MA, USA, 2001; ISBN 978-0-7923-8425-0.
54. Çengel, Y.A.; Boles, M.A.; Kanoğlu, M. *Thermodynamics: An Engineering Approach*, 9th ed.; McGraw-Hill Education: New York, NY, USA, 2019; ISBN 978-1-259-82267-4.
55. Haji Abolhasani, M.; Safavi, M.; Goodarzi, M.T.; Kassaei, S.M.; Azin, M. Statistical Optimization of Medium with Response Surface Methodology for Biomass Production of a Local Iranian Microalgae *Picochlorum* sp. RCC486. *Adv. Res. Microb. Metab. Technol.* **2018**, *1*, 39–49. [\[CrossRef\]](#)
56. Cheadle, C.; Vawter, M.P.; Freed, W.J.; Becker, K.G. Analysis of Microarray Data Using Z Score Transformation. *J. Mol. Diagn.* **2003**, *5*, 73–81. [\[CrossRef\]](#) [\[PubMed\]](#)
57. Wang, B. A Zipf-Plot Based Normalization Method for High-Throughput RNA-Seq Data. *PLoS ONE* **2020**, *15*, e0230594. [\[CrossRef\]](#)
58. Becker, E.W. Micro-Algae as a Source of Protein. *Biotechnol. Adv.* **2007**, *25*, 207–210. [\[CrossRef\]](#) [\[PubMed\]](#)
59. Wang, L.; Li, Y.; Chen, P.; Min, M.; Chen, Y.; Zhu, J.; Ruan, R.R. Anaerobic Digested Dairy Manure as a Nutrient Supplement for Cultivation of Oil-Rich Green Microalgae *Chlorella* sp. *Bioresour. Technol.* **2010**, *101*, 2623–2628. [\[CrossRef\]](#) [\[PubMed\]](#)
60. Illman, A.M.; Scragg, A.H.; Shales, S.W. Increase in *Chlorella* Strains Calorific Values When Grown in Low Nitrogen Medium. *Enzyme Microb. Technol.* **2000**, *27*, 631–635. [\[CrossRef\]](#)
61. Feng, P.; Deng, Z.; Fan, L.; Hu, Z. Lipid Accumulation and Growth Characteristics of *Chlorella zofingiensis* under Different Nitrate and Phosphate Concentrations. *J. Biosci. Bioeng.* **2012**, *114*, 405–410. [\[CrossRef\]](#)
62. Griffiths, M.J.; Harrison, S.T.L. Lipid Productivity as a Key Characteristic for Choosing Algal Species for Biodiesel Production. *J. Appl. Phycol.* **2009**, *21*, 493–507. [\[CrossRef\]](#)
63. Ziganshina, E.E.; Bulynina, S.S.; Ziganshin, A.M. Growth Characteristics of *Chlorella Sorokiniana* in a Photobioreactor during the Utilization of Different Forms of Nitrogen at Various Temperatures. *Plants* **2022**, *11*, 1086. [\[CrossRef\]](#)
64. Koutra, E.; Mastropetros, S.G.; Ali, S.S.; Tsigkou, K.; Kornaros, M. Assessing the Potential of *Chlorella vulgaris* for Valorization of Liquid Digestates from Agro-Industrial and Municipal Organic Wastes in a Biorefinery Approach. *J. Clean. Prod.* **2021**, *280*, 124352. [\[CrossRef\]](#)
65. Mastropetros, S.G.; Koutra, E.; Amouri, M.; Aziza, M.; Ali, S.S.; Kornaros, M. Comparative Assessment of Nitrogen Concentration Effect on Microalgal Growth and Biochemical Characteristics of Two *Chlorella* Strains Cultivated in Digestate. *Mar. Drugs* **2022**, *20*, 415. [\[CrossRef\]](#)
66. Choix, F.J.; de-Bashan, L.E.; Bashan, Y. Enhanced Accumulation of Starch and Total Carbohydrates in Alginate-Immobilized *Chlorella* spp. Induced by Azospirillum Brasilense: II. Heterotrophic Conditions. *Enzyme Microb. Technol.* **2012**, *51*, 300–309. [\[CrossRef\]](#) [\[PubMed\]](#)
67. Cheng, D.; Li, D.; Yuan, Y.; Zhou, L.; Li, X.; Wu, T.; Wang, L.; Zhao, Q.; Wei, W.; Sun, Y. Improving Carbohydrate and Starch Accumulation in *Chlorella* sp. AE10 by a Novel Two-Stage Process with Cell Dilution. *Biotechnol. Biofuels* **2017**, *10*, 75. [\[CrossRef\]](#)
68. Sharma, K.K.; Schuhmann, H.; Schenk, P.M. High Lipid Induction in Microalgae for Biodiesel Production. *Energies* **2012**, *5*, 1532–1553. [\[CrossRef\]](#)
69. Ho, S.-H.; Huang, S.-W.; Chen, C.-Y.; Hasunuma, T.; Kondo, A.; Chang, J.-S. Characterization and Optimization of Carbohydrate Production from an Indigenous Microalga *Chlorella vulgaris* FSP-E. *Bioresour. Technol.* **2013**, *135*, 157–165. [\[CrossRef\]](#) [\[PubMed\]](#)
70. Ho, S.-H.; Chen, C.-Y.; Chang, J.-S. Effect of Light Intensity and Nitrogen Starvation on CO₂ Fixation and Lipid/Carbohydrate Production of an Indigenous Microalga *Scenedesmus Obliquus* CNW-N. *Bioresour. Technol.* **2012**, *113*, 244–252. [\[CrossRef\]](#)
71. Chia, M.A.; Lombardi, A.T.; da Graça Gama Melão, M.; Parrish, C.C. Combined Nitrogen Limitation and Cadmium Stress Stimulate Total Carbohydrates, Lipids, Protein and Amino Acid Accumulation in *Chlorella vulgaris* (Trebouxiophyceae). *Aquat. Toxicol.* **2015**, *160*, 87–95. [\[CrossRef\]](#) [\[PubMed\]](#)
72. Tale, M.P.; Devi Singh, R.; Kapadnis, B.P.; Ghosh, S.B. Effect of Gamma Irradiation on Lipid Accumulation and Expression of Regulatory Genes Involved in Lipid Biosynthesis in *Chlorella* sp. *J. Appl. Phycol.* **2018**, *30*, 277–286. [\[CrossRef\]](#)
73. Xia, A.; Murphy, J.D. Microalgal Cultivation in Treating Liquid Digestate from Biogas Systems. *Trends Biotechnol.* **2016**, *34*, 264–275. [\[CrossRef\]](#)

74. Nwoba, E.G.; Mickan, B.S.; Moheimani, N.R. *Chlorella* sp. Growth under Batch and Fed-Batch Conditions with Effluent Recycling When Treating the Effluent of Food Waste Anaerobic Digestate. *J. Appl. Phycol.* **2019**, *31*, 3545–3556. [\[CrossRef\]](#)
75. Zhu, L.; Yan, C.; Li, Z. Microalgal Cultivation with Biogas Slurry for Biofuel Production. *Bioresour. Technol.* **2016**, *220*, 629–636. [\[CrossRef\]](#)
76. Ali, H.E.A.; El-fayoumy, E.A.; Rasmy, W.E.; Soliman, R.M.; Abdullah, M.A. Two-Stage Cultivation of *Chlorella vulgaris* Using Light and Salt Stress Conditions for Simultaneous Production of Lipid, Carotenoids, and Antioxidants. *J. Appl. Phycol.* **2021**, *33*, 227–239. [\[CrossRef\]](#)
77. Yadav, D.K.; Yadav, M.; Rani, P.; Yadav, A.; Bhardwaj, N.; Bishnoi, N.R.; Singh, A. Screening of Best Growth Media for *Chlorella vulgaris* Cultivation and Biodiesel Production. *Biofuels* **2024**, *15*, 271–277. [\[CrossRef\]](#)
78. Morowvat, M.H.; Ghasemi, Y. Cell Growth, Lipid Production and Productivity in Photosynthetic Microalga *Chlorella vulgaris* under Different Nitrogen Concentrations and Culture Media Replacement. *Recent Pat. Food Nutr. Agric.* **2018**, *9*, 142–151. [\[CrossRef\]](#)
79. Dahiya, S.; Chowdhury, R.; Tao, W.; Kumar, P. Biomass and Lipid Productivity by Two Algal Strains of *Chlorella Sorokiniana* Grown in Hydrolysate of Water Hyacinth. *Energies* **2021**, *14*, 1411. [\[CrossRef\]](#)
80. Mohan Singh, H.; Tyagi, V.V.; Kothari, R.; Azam, R.; Singh Slathia, P.; Singh, B. Bioprocessing of Cultivated *Chlorella Pyrenoidosa* on Poultry Excreta Leachate to Enhance Algal Biomolecule Profile for Resource Recovery. *Bioresour. Technol.* **2020**, *316*, 123850. [\[CrossRef\]](#)
81. Vishwakarma, R.; Dhar, D.W.; Saxena, S. Influence of Nutrient Formulations on Growth, Lipid Yield, Carbon Partitioning and Biodiesel Quality Potential of *Botryococcus* sp. and *Chlorella* sp. *Environ. Sci. Pollut. Res.* **2019**, *26*, 7589–7600. [\[CrossRef\]](#)
82. Zhang, L.; Cheng, J.; Pei, H.; Pan, J.; Jiang, L.; Hou, Q.; Han, F. Cultivation of Microalgae Using Anaerobically Digested Effluent from Kitchen Waste as a Nutrient Source for Biodiesel Production. *Renew. Energy* **2018**, *115*, 276–287. [\[CrossRef\]](#)
83. Magdaong, J.B.; Ubando, A.T.; Culaba, A.B.; Chang, J.S.; Chen, W.H. Effect of Aeration Rate and Light Cycle on the Growth Characteristics of *Chlorella Sorokiniana* in a Photobioreactor. *IOP Conf. Ser. Earth Environ. Sci.* **2019**, *268*, 012112. [\[CrossRef\]](#)
84. Chai, S.; Shi, J.; Huang, T.; Guo, Y.; Wei, J.; Guo, M.; Li, L.; Dou, S.; Liu, L.; Liu, G. Characterization of *Chlorella Sorokiniana* Growth Properties in Monosaccharide-Supplemented Batch Culture. *PLoS ONE* **2018**, *13*, e0199873. [\[CrossRef\]](#)
85. Zhu, Q.; Zhang, M.; Liu, B.; Wen, F.; Yang, Z.; Liu, J. Transcriptome and Metabolome Profiling of a Novel Isolate *Chlorella Sorokiniana* G32 (Chlorophyta) Displaying Enhanced Starch Accumulation at High Growth Rate Under Mixotrophic Condition. *Front. Microbiol.* **2022**, *12*, 760307. [\[CrossRef\]](#)
86. Cecchin, M.; Benfatto, S.; Griggio, F.; Mori, A.; Cazzaniga, S.; Vitulo, N.; Delledonne, M.; Ballottari, M. Molecular Basis of Autotrophic vs Mixotrophic Growth in *Chlorella Sorokiniana*. *Sci. Rep.* **2018**, *8*, 6465. [\[CrossRef\]](#) [\[PubMed\]](#)
87. Zhang, L.; Pei, H.; Chen, S.; Jiang, L.; Hou, Q.; Yang, Z.; Yu, Z. Salinity-Induced Cellular Cross-Talk in Carbon Partitioning Reveals Starch-to-Lipid Biosynthesis Switching in Low-Starch Freshwater Algae. *Bioresour. Technol.* **2018**, *250*, 449–456. [\[CrossRef\]](#) [\[PubMed\]](#)
88. El-Adl, M.; Deyab, M.A.; Khafaga, M.M.; Ahmed, S.E.-S.A. The Freshwater Alga *Chlorella Sorokiniana* Tolerates Salt Stress via Modulating Metabolites and Minerals. *Sci. J. Damietta Fac. Sci.* **2024**, *14*, 44–51. [\[CrossRef\]](#)
89. Yun, C.-J.; Hwang, K.-O.; Han, S.-S.; Ri, H.-G. The Effect of Salinity Stress on the Biofuel Production Potential of Freshwater Microalgae *Chlorella vulgaris* YH703. *Biomass Bioenergy* **2019**, *127*, 105277. [\[CrossRef\]](#)
90. Li, H.; Tan, J.; Mu, Y.; Gao, J. Lipid Accumulation of *Chlorella* sp. TLD6B from the Taklimakan Desert under Salt Stress. *PeerJ* **2021**, *9*, e11525. [\[CrossRef\]](#)
91. Juneja, A.; Ceballos, R.; Murthy, G. Effects of Environmental Factors and Nutrient Availability on the Biochemical Composition of Algae for Biofuels Production: A Review. *Energies* **2013**, *6*, 4607–4638. [\[CrossRef\]](#)
92. Miao, X.; Wu, Q. Biodiesel Production from Heterotrophic Microalgal Oil. *Bioresour. Technol.* **2006**, *97*, 841–846. [\[CrossRef\]](#)
93. Liu, J.; Huang, J.; Sun, Z.; Zhong, Y.; Jiang, Y.; Chen, F. Differential Lipid and Fatty Acid Profiles of Photoautotrophic and Heterotrophic *Chlorella zofingiensis*: Assessment of Algal Oils for Biodiesel Production. *Bioresour. Technol.* **2011**, *102*, 106–110. [\[CrossRef\]](#)
94. Talebi, A.F.; Mohtashami, S.K.; Tabatabaei, M.; Tohidfar, M.; Bagheri, A.; Zeinalabedini, M.; Hadavand Mirzaei, H.; Mirzajanzadeh, M.; Malekzadeh Shafaroudi, S.; Bakhtiari, S. Fatty Acids Profiling: A Selective Criterion for Screening Microalgae Strains for Biodiesel Production. *Algal Res.* **2013**, *2*, 258–267. [\[CrossRef\]](#)
95. Knothe, G. “Designer” Biodiesel: Optimizing Fatty Ester Composition to Improve Fuel Properties. *Energy Fuels* **2008**, *22*, 1358–1364. [\[CrossRef\]](#)
96. Menegazzo, M.L.; Ulusoy-Erol, H.B.; Hestekin, C.N.; Hestekin, J.A.; Fonseca, G.G. Evaluation of the Yield, Productivity, and Composition of Fatty Acids Methyl Esters (FAME) Obtained from the Lipidic Fractions Extracted from *Chlorella Sorokiniana* by Using Ultrasound and Agitation Combined with Solvents. *Biofuels* **2022**, *13*, 519–526. [\[CrossRef\]](#)
97. Wang, M.; Sahu, A.K.; Rusten, B.; Park, C. Anaerobic Co-Digestion of Microalgae *Chlorella* sp. and Waste Activated Sludge. *Bioresour. Technol.* **2013**, *142*, 585–590. [\[CrossRef\]](#) [\[PubMed\]](#)

98. González-Fernández, C.; Sialve, B.; Bernet, N.; Steyer, J.P. Thermal Pretreatment to Improve Methane Production of *Scenedesmus* Biomass. *Biomass Bioenergy* **2012**, *40*, 105–111. [\[CrossRef\]](#)
99. Sialve, B.; Bernet, N.; Bernard, O. Anaerobic Digestion of Microalgae as a Necessary Step to Make Microalgal Biodiesel Sustainable. *Biotechnol. Adv.* **2009**, *27*, 409–416. [\[CrossRef\]](#) [\[PubMed\]](#)
100. Rambo, I.M.; Dombrowski, N.; Constant, L.; Erdner, D.; Baker, B.J. Metabolic Relationships of Uncultured Bacteria Associated with the Microalgae *Gambierdiscus*. *Environ. Microbiol.* **2020**, *22*, 1764–1783. [\[CrossRef\]](#)
101. Wang, M.; Kuo-Dahab, W.C.; Dolan, S.; Park, C. Kinetics of Nutrient Removal and Expression of Extracellular Polymeric Substances of the Microalgae, *Chlorella* sp. and *Micractinium* sp., in Wastewater Treatment. *Bioresour. Technol.* **2014**, *154*, 131–137. [\[CrossRef\]](#)
102. Mendez, L.; Mahdy, A.; Timmers, R.A.; Ballesteros, M.; González-Fernández, C. Enhancing Methane Production of *Chlorella vulgaris* via Thermochemical Pretreatments. *Bioresour. Technol.* **2013**, *149*, 136–141. [\[CrossRef\]](#)
103. Passos, F.; Ferrer, I. Influence of Hydrothermal Pretreatment on Microalgal Biomass Anaerobic Digestion and Bioenergy Production. *Water Res.* **2015**, *68*, 364–373. [\[CrossRef\]](#)
104. Williams, P.J.I.B.; Laurens, L.M.L. Microalgae as Biodiesel & Biomass Feedstocks: Review & Analysis of the Biochemistry, Energetics & Economics. *Energy Environ. Sci.* **2010**, *3*, 554–590. [\[CrossRef\]](#)
105. Ramanan, R.; Kim, B.-H.; Cho, D.-H.; Oh, H.-M.; Kim, H.-S. Algae–Bacteria Interactions: Evolution, Ecology and Emerging Applications. *Biotechnol. Adv.* **2016**, *34*, 14–29. [\[CrossRef\]](#)

Disclaimer/Publisher’s Note: The statements, opinions and data contained in all publications are solely those of the individual author(s) and contributor(s) and not of MDPI and/or the editor(s). MDPI and/or the editor(s) disclaim responsibility for any injury to people or property resulting from any ideas, methods, instructions or products referred to in the content.